

# **Design of the Drive System and Battery Cage for the 2009 REV FSAE Vehicle**



**Marius Ivanescu**

Student Number: 10426636

School of Mechanical Engineering, University of Western Australia

**Supervisor: Dr. Kamy Cheng**

School of Mechanical Engineering, University of Western Australia

**Co-Supervisor: Dr. Thomas Bräunl**

School of Electrical & Computer Engineering, University of Western Australia

**Final Year Project Thesis**

**School of Mechanical Engineering**

**University of Western Australia**

**Submitted: October 26th, 2009**

## Synopsis

The 2001 UWA Formula SAE (Society of Automotive Engineers) Motorsport vehicle was converted to an electric drive system by the Renewable Energy Vehicle (REV) team for the upcoming Formula SAE student design competition. The aim of this project was to research and design a battery restraint system and a drive mechanism to power the converted 2001 UWA Motorsport vehicle.

A waterproof and visually open design for the battery cage was produced attempting to adhere to the national code of practice for the construction and modification of light vehicles. The model was produced in Solidworks before being stress analysed in ANSYS Workbench.

The initially imposed drive mechanism was that of a wheel hub motor. An analysis of the performance requirements determined that 20kW of power and 120Nm of torque were required. Attempts made to source a suitably powerful electric motor that would be able to fit within the current arrangement as the constrained budget did not allow for major modification to the existing vehicle. This led to the Plettenberg Predator, a brushless DC large scale model aircraft motor, however the required supporting structure confirmed through stress analysis with ANSYS Workbench was heavy and had a high part count due to the necessary reduction ratio and belt load. Additionally, it could not be designed within the budget and time constraints to fully protect the motor from overheating and vibration, which were identified as the primary failure modes of the electric motor outside of their intended application.

The arbitrary wheel hub drive mechanism requirement was lifted and an inboard solution sought. This was using two brushless DC pancake motors and a plate style modular single stage arrangement that could be fully removed from the vehicle for modification and testing. This type of arrangement still has the advantage of fully independent rear wheel control; however the motor was inboard as sprung mass and fully enclosed for protection. Custom pulleys and adjustable idlers needed to be designed and manufactured, as well as modifications to CV joints and drive shafts to support the new design.





Marius Ivanescu  
194 Holmes Road  
Forrestfield, WA, 6058

26th October, 2009

Professor David Smith  
Dean  
Faculty of Engineering, Computing and Mathematics  
University of Western Australia  
35 Stirling Highway  
Crawley, WA, 6009

Dear Professor Smith

I am pleased to submit this thesis, entitled “Design of the Drive System and Battery Cage for the 2009 REV FSAE Vehicle”, as part of the requirement for the degree of Bachelor of Engineering.

Yours Sincerely

Marius Ivanescu

10426636

I would like to thank Chris Rowles and Lynn Kirkham for their warm-hearted support and technical guidance for the duration of the project. I am also indebted to Lachlan Tomlin for donating the vehicle and the countless hours spent generating the chassis CAD drawings and rebuilding the vehicle for the REV FSAE team.

## Table of Contents

1. Vehicle Background.....	1
1.1 Managing Delay.....	2
1.2 Group Meetings.....	2
2. Battery Cage Design .....	3
2.1 REV Getz & Elise .....	3
2.2 REV FSAE Vehicle Requirements .....	4
2.2.1 Battery Characteristics.....	4
2.3 Design Development.....	6
2.3.1 Materials .....	7
2.3.2 Design & Assembly.....	7
2.3.3 Waterproofing .....	8
2.4 Battery Cage Stress Analysis.....	9
2.4.1 Model Refinement .....	10
2.5 Manufacturing.....	13
2.6 Evaluation & Future Work .....	14
3. Wheel Hub Motor .....	15
3.1 Background.....	15
3.1.1 Siemens VDO eCorner .....	16
3.1.2 Michelin Active Wheel.....	17
3.1.3 Hi-Pa Drive .....	18
3.2 REV FSAE Wheel Hub Motor .....	19
3.3 Requirements .....	20
3.4 Motor Selection.....	20
3.5 BLDC Outrunner Issues .....	24
3.5.1 Limited Start-up Torque .....	24
3.5.2 Overheating.....	25
3.5.3 Inboard Appeal.....	25
3.6 Reduction Mechanism.....	26
3.6.1 Chain and Sprocket.....	26
3.6.2 Spur Gears.....	27
3.6.3 Planetary Gears .....	28
3.6.4 Synchronous Pulley and Belt .....	30
3.7 Rudimentary Design Process.....	30

3.7.1 Design Development .....	31
3.7.2 Two Stage Phase 1.....	31
3.7.3 Two Stage Phase 2.....	33
3.7.4 Two Stage Phase 3.....	35
3.7.5 Two Stage Phase 4.....	35
3.7.6 Two Stage Phase 5.....	36
3.8 Two Stage Stress Analysis .....	37
3.9 Two Stage Design Evaluation.....	40
3.10 Single Stage Design.....	40
3.10.1 Single Stage Stress Analysis .....	41
3.11 Future Work.....	43
3.12 Postponement of Wheel Hub Concept .....	44
4. Inboard Drive Design.....	45
4.1 Adjacent Two Stage .....	47
4.2 Inline Phase 1 .....	48
4.3 Inline Phase 1 Stress Analysis .....	49
4.3.1 Refinement of Inline Phase 1 .....	52
4.4 Inline Phase 2.....	54
4.5 Inline Phase 2 Stress Analysis .....	56
4.6 Bearing Selection .....	58
4.7 Pulley & Belt Selection .....	59
4.8 Drive shafts & CV Joints.....	61
4.9 Evaluation .....	63
4.10 Future Work.....	64
4.11 Safety.....	64
5 UWAM and REV FSAE .....	65
6. References .....	67
Appendix .....	71
A: Battery Cage .....	71
B: Structural Steel Strength Certification.....	72
C: Exploded View of Wheel Hub Design .....	73
D: Inboard Design.....	75
E: Exploded View of Inboard.....	77
F: Pulley & Idler .....	78

## 1. Vehicle Background

The UWA Motorsport team (UWAM) was formed in 2001 and competed in their first Formula SAE (Society of Automotive Engineers) student design competition with great success. The vehicle produced for that first UWAM build was donated to the REV (Renewable Energy Vehicle) FSAE team eight years later and formed the base of the 2009 REV FSAE vehicle.

After taking on the project at the beginning of semester the scope of the project was defined and sub-projects were assigned to group members by the author acting as team leader, based on member's interest and previous experience.

This was loosely divided into the following subtasks:

- **Suspension** - analysis of the 2001 petrol setup and assessment of the impact of changes in weight due to the electric conversion.
- **Battery cage and chassis** – the electric conversion of the vehicle required the design and analysis of a battery cage, and the stress analysis of the updated chassis.
- **Drive mechanism** – based on the power and torque requirements, design and manufacture of a drive mechanism.
- **Vehicle dynamics** – assess the steering, stability and weight distribution due to the electric conversion.
- **Electrical** – determine battery requirements as per the competition requirements and motor controller selection.
- **Instrumentation** – design of the steering and traction control systems.

There was significant overlap between assigned roles and students were expected to share information and work together. Students were given subtasks, short and long-term goals to maintain motivation and direction.

### 1.1 Managing Delay

When the project commenced the understanding between the Mechanical and Electrical Engineering departments was that a rolling chassis would be complete and available at the beginning of semester so that students could work on it as their final year projects and produce an electric vehicle for the end of year FSAE competition to be held in Melbourne. However there was a month long delay in getting the parts to the university, after which only the suspension and uprights were found. Three months would pass before the chassis was finally welded and a mock assembly available to students. This was then followed by a month during which the chassis needed to be sandblasted, primed and painted and the whole vehicle assembled for final takeover by the REV FSAE group.

During the early phase when the chassis and parts were unavailable, time was spent researching and conducting a literature review. When the suspension was made available the initial designs were refined and feedback sought from technicians and workshop staff as to the design suitability. When the whole vehicle was finally available, those in vehicle dynamics and battery cage were able to carry out their tasks and put their designs into practice. Offers were made by students to assist in the rebuild to increase their knowledge of the assembly and maintenance of the vehicle.

### 1.2 Group Meetings

Meetings were held twice weekly to assess individual and project progress. A formal group presentation was held weekly on Mondays detailing the progress made during the previous week and tasks required for the following week. Weekly informal meetings were also held in the workshop with the vehicle to aid in visualising and discussing technical problems with workshop staff.

Students were required to attend safety inductions for all labs in which they worked including electrical and mechanical workshops, and the motorsport area. Students were not permitted in the workshop unattended after hours in case of an accident that required assistance.

## 2. Battery Cage Design

This section describes the requirements, design, manufacture and evaluation of the battery restraint system developed for the 2009 REV FSAE vehicle.

### 2.1 REV Getz & Elise

The first REV electric conversion vehicle was a Hyundai Getz and as a road going vehicle the battery cage was designed as per the National Code of Practice (NCOP) for Light Vehicle Construction and Modification (Department of Infrastructure, Transport, Regional Development and Local Government 2006). This required a 20-g front impact, 15-g side impact and 10-g rear and vertical. The battery cage, shown in figure 2.1-1 was a single unit manufactured from a combination of steel angle and tubing to reduce the weight while keeping the strength high. The unit contained the batteries, battery management system units (BMS) and ancillary electrical equipment (Ip 2008).



Figure 2.1-1: Getz battery cage in the boot of the vehicle.

The battery restraint system developed for the Lotus Elise was separated to three units that contained only batteries: ancillary electrical equipment had its own separate enclosure (Tietzel 2009). The three cages were designed to the same impact loading as the Getz, but used only angle rather than tubing so that a smaller structure could be achieved. This project applies the principles developed by Tietzel for the battery cage design during the conversion of the Lotus Elise.

## 2.2 REV FSAE Vehicle Requirements

The design of the REV FSAE vehicle battery cage had to fulfil several requirements:

- Accommodate 15 Thunder Sky TS-LFP90AHA cells decided upon by the REV electrical group.
- Waterproofed to withstand a direct water jet from all directions for 30 seconds to be accepted into the FSAE competition.
- Accommodate battery management system units (BMS) between the batteries at a height of up to 30mm over the cell terminals, as well as the battery connector.
- Easily manufacturable to align with the competition philosophy of producing a vehicle that can be mass produced for below \$25,000.
- The top of the batteries must be visually accessible to inspect the BMS LED indicators. The batteries must also be physically removable for testing and replacement.

### *2.2.1 Battery Characteristics*

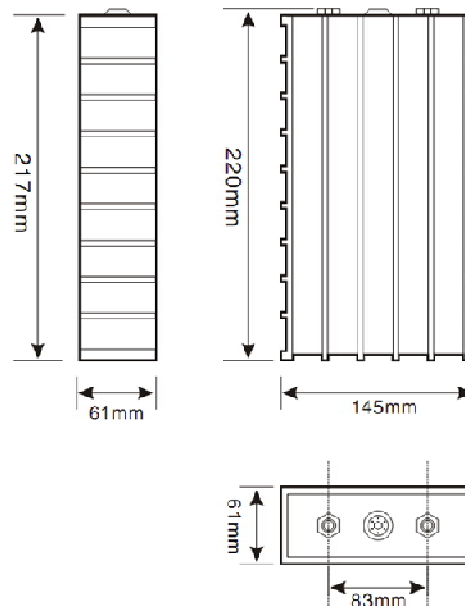


Figure 2.2.1-1: Thunder Sky 90Ah battery dimensions. (Thunder Sky 2009)

The batteries used are hermetically sealed with ribbed, plastic prismatic casing and are fitted with safety vents for protection against rupture. 15 batteries each weighing  $3\text{kg} \pm 0.1$  each were used.



The issue of heat generation was investigated prior to battery selection and it was confirmed with the supplier that the batteries do not need active cooling as their operating temperature range is  $-45^{\circ}$  to  $85^{\circ}$  (Thunder Sky 2009) which could be maintained by passive heat dissipation from the cage under normal loading, while the battery casing is durable up to  $250^{\circ}\text{C}$ .

Real world performance and testing will be required to adequately determine the need for active cooling as there will be a higher current demand from the batteries exceeding the nominal value in the documentation.

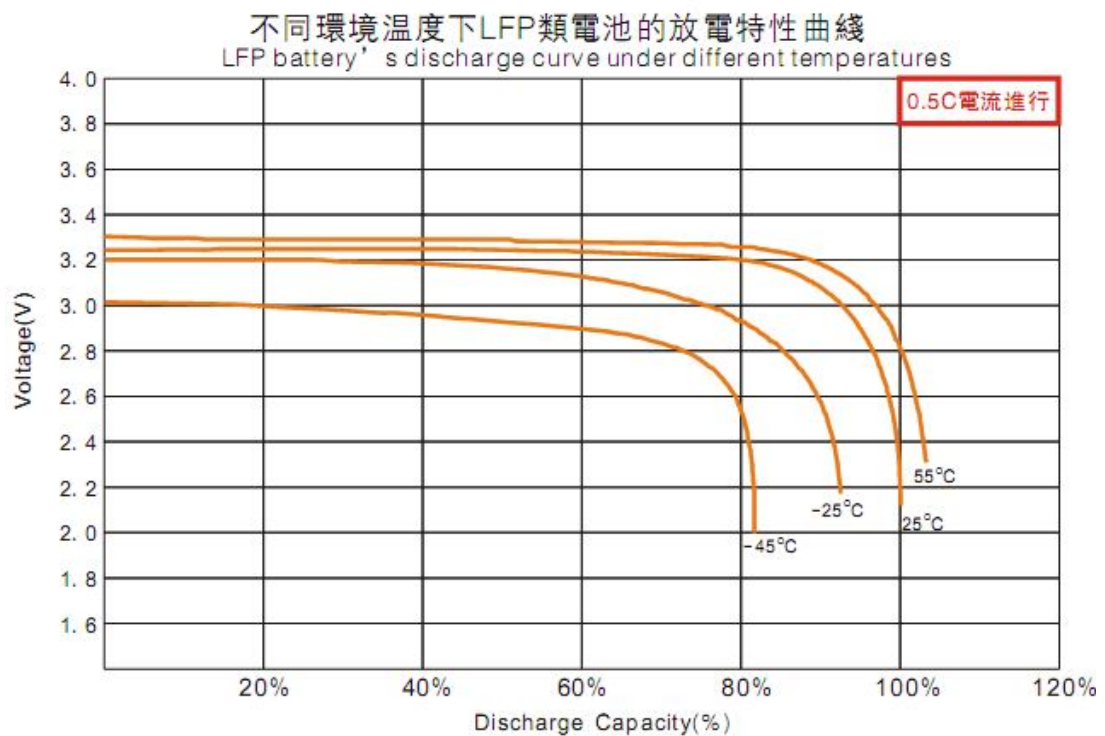


Figure 2.2.1-2: Discharge voltage of the 90Ah batteries for various temperature and discharge capacities (Thunder Sky 2009).

Ideally the batteries will be maintained at  $60^{\circ}\text{C}$  during use to a maximum discharge capacity of 80% as shown in figure 2.2.1-2 in order to deliver the highest voltage while still preserving the life of the battery.

### 2.3 Design Development

There was no guidance in the Formula Hybrid Competition rules (Formula Hybrid 2009a) regarding strength and impact requirements for the battery cage. Structural requirements have been met by the chassis design, and electrical safety requirements by the electrical group as per the competition standards (Formula Hybrid 2009b). The mechanical design of the battery cage was at the discretion of the student engineer and attempted to use the NCOP best practice for guidance in the relative proportions of front, side and rear and vertical impact loadings.

The development of the battery cage was an iterative process with practical feedback from the electrical and mechanical workshop staff, as well as the theoretical results of the stress analysis. The concept was decided upon that met all the requirements before CAD drawings were produced in Solidworks '08 and imported into ANSYS Workbench for optimisation.

During the chassis modification the optimal battery cage position was found to be behind the driver's seat as shown in figure 2.3-1, in the place of the original motor (Corke 2009).



Figure 2.3-1: Proposed battery cage location behind driver seat.

This satisfied the electrical group for easy and central access, as well as vehicle dynamics (Morrigan 2009) so that the weight distribution of the car was not greatly modified from the original petrol setup.

### *2.3.1 Materials*

Both structural steel and aluminium were investigated as potential materials for battery cage construction. Aluminium required additional material to meet the same strength requirements as steel which resulted in difficulty packaging the cage at the narrow rear of the vehicle. Angle structural steel with a yield strength of 320MPa and an ultimate tensile stress of 440MPa (Appendix B) was chosen for its higher strength for the same volume when compared to aluminium.

### *2.3.2 Design & Assembly*

Practical designs were first hand sketched before a scale model of the battery cage was made of cardboard to ensure that it could be easily removed and did not clash with the seat and chassis. This practical method was faster than attempting to visualise on paper or modelling in Solidworks. The initial box was refined and additional support members added at its base to increase the strength and reduce deflection, as discussed in the next section.

Additional parts, shown in figure 2.3.2-1, were required to fix the batteries into place so they did not move vertically in the cage. This was achieved with rubber stoppers that would be fixed to the top straps and push down on the edges of the batteries. A thin foam layer was added between the batteries and the aluminium side sheet to take up any lateral motion.

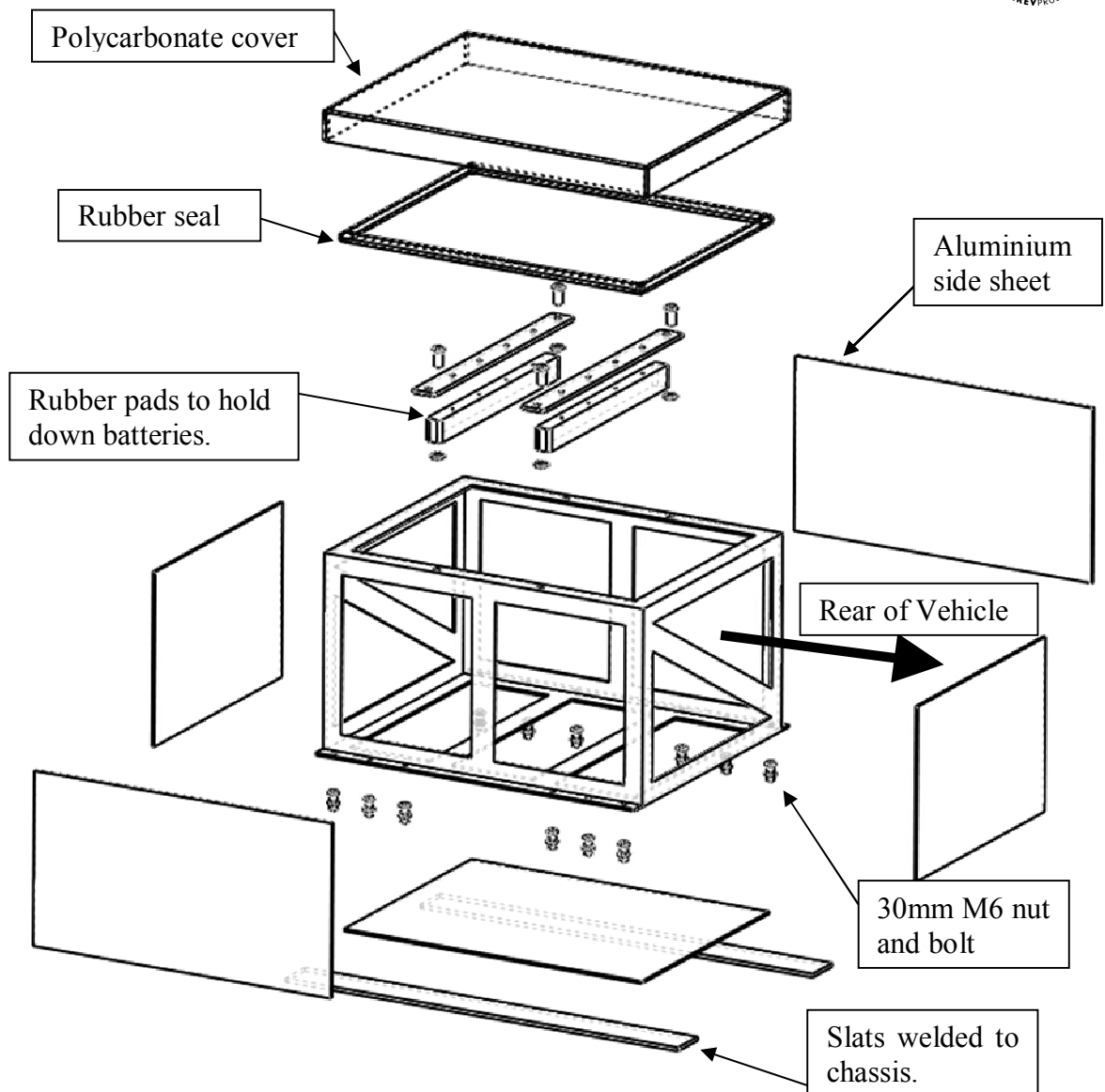


Figure 2.3.2-1: Exploded view of all components in the battery cage assembly. Aluminium sheets are shown outside the cage for simplicity but are sealed on the inside.

### 2.3.3 Waterproofing

Both plastic and aluminium sheets were considered to waterproof the structure. Aluminium sheet of 1.6mm thickness was chosen because of its superior thermal conductivity of  $237 \text{ Wm}^{-1}\text{K}^{-1}$  (Callister 2007) over plastic. This would aid heat dissipation from the batteries and reduce the future need for active cooling. Waterproofing was achieved using aluminium sheet sealed to the inside of the cage structure with silicon on all sides except the top.

Waterproofing the top of the structure was complicated by the need for physical and visual access to the batteries. The top casing needed to be transparent so that the BMS units between each cells could be viewed. The cover also needed to be removable to allow access to the batteries for service and replacement. This was achieved using clear polycarbonate with a rubber seal as shown in figure 2.3.2-1. This is heat resistant up to 125°C and has high impact resistance (Callister 2007). The intention was to package the fuse, contactor and cable connector with the batteries so that only one unit needed to be sealed against water. After reviewing the dimensions of this arrangement it was found that it would result in complex geometry, increasing the manufacturing price of both battery cage and waterproofing lid so they were sealed in a separate unit that did not require stress analysis.

#### 2.4 Battery Cage Stress Analysis

A static analysis of the battery cage was performed in ANSYS Workbench by importing the Solidworks CAD files and applying loads to simulate worst-case scenarios.

The NCOP guidelines are designed for road registered vehicles, not FSAE Hybrid vehicles. Additionally, the chassis has been designed and stress analysed to meet the FSAE competition standards. As a result, the full side and rear impact loading according to the NCOP guideline was not used as it would have resulted in an excessively heavy structure not suitable for the performance application. The guideline was instead used for relative proportions between rear, side and vertical impact.

A 5,000N static force was used to simulate side impact loading. As the battery cage was not a structural member of the chassis and the battery cage would be shielded by the chassis during an impact, this figure was considered adequate. This force was divided by the area and applied as a pressure to the whole side of the structure. A force of 2500N was similarly applied to the rear of the battery cage, and 5000N vertically.

A non-linear analysis was performed using a free mesh generated by ANSYS with attention focused on the areas of potentially high stress concentration such as changes in direction and tight radiuses. Analyses were performed with the *large deflection* and *aggressive mechanical* options as the analysis focuses on the ultimate tensile strength and large deflections of the cage in the case of an impact. Once a satisfactory model was

developed, a convergence test was performed with the side impact loading scenario such that the difference in the von-Mises equivalent stress values was below 5% for variations in mesh resolution.

The slats across the top of the cage were used in the analysis with a bonded contact type in ANSYS. This assumes that the bolt holding down the slat applies a force large enough for the friction between slat and cage to act as a single unit.

The stress analysis was performed without the batteries in place, reducing the rigidity of the model compared to the physical structure which would always contain batteries when in use. The weight of the batteries was not used in the analysis as the dynamic issue of the batteries bouncing in their enclosure was solved by the rubber stoppers that held the batteries in place, and the force of battery weight was small when compared to the applied force during a side impact.

#### 2.4.1 Model Refinement

The bolt holes were first simulated as a cylindrically fixed point in space, however this resulted in high and unrealistic stress concentration around the bolt holes as shown in figure 2.4.1-1. This type of restraint did not allow for any deformation of the material around the bolt holes, which did not accurately reflect the physical situation leading to high stress value. To overcome this, the 12 bolt holes were removed and replaced in the model by a 12 single points fixed in space.

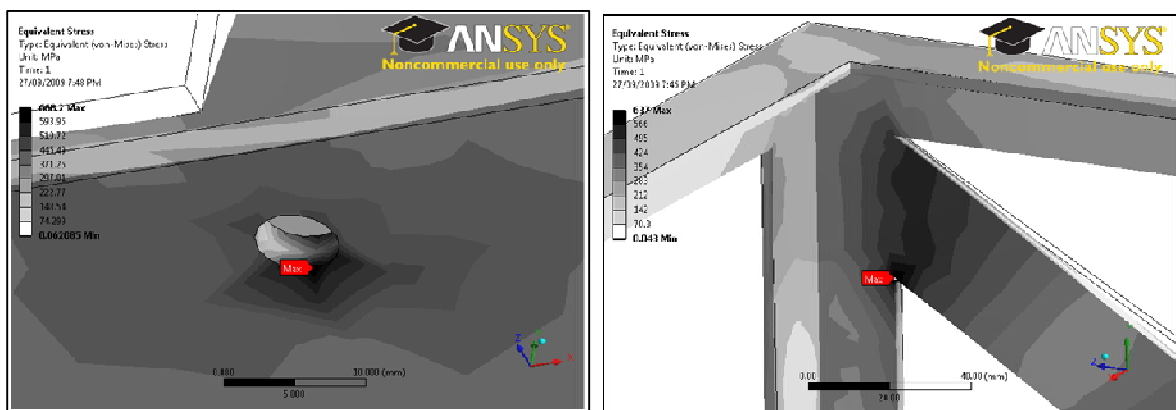


Figure 2.4.1-1: Left - unrealistic stress concentrations due to cylindrical fixed support; right - sharp corners.

Modifications needed to be made to the cage from the initial design to reduce the sharp corners that were leading to stress concentrations shown in figure 2.4.1-1. Stress values

in excess of the 440MPa ultimate strength of the material were experienced so a 5mm fillet radius was added at the acute corners.

Both side and rear impact scenarios were tested and the structure further developed and reinforced so that either side impact or rear impact was below the 440MPa ultimate strength of the material. The combination effect of side, rear and vertical impact was not analysed as it was considered an unrealistic scenario that would have resulted in an excessively reinforced structure for the application.

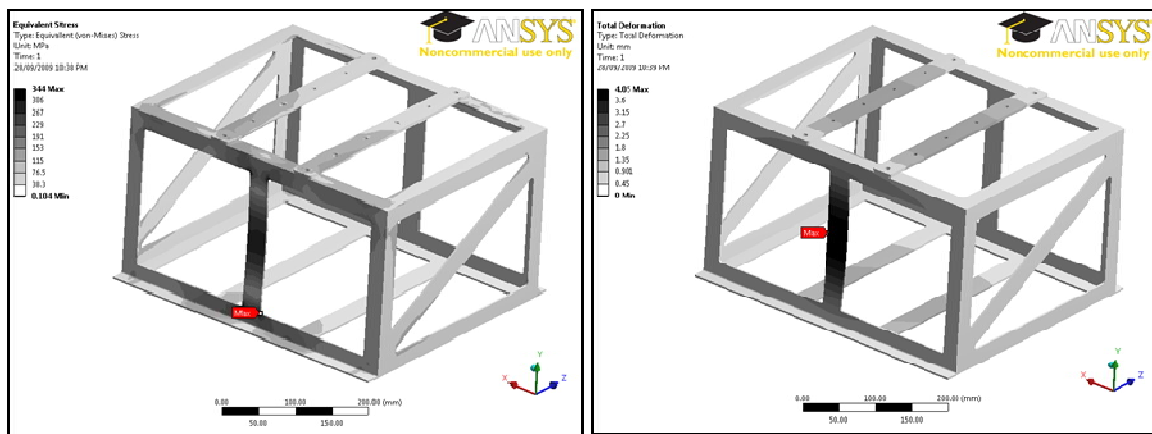


Figure 2.4.1-2: Left - side impact von Mises equivalent stress contour plot and right - deflection contour plot.

Figure 2.4.1-2 shows the side stress and deflection contour plots of a side impact. The maximum von-Mises equivalent stress of 344MPa occurs at the tight radius change while the maximum deflection of 4mm is at the least supported centre section.

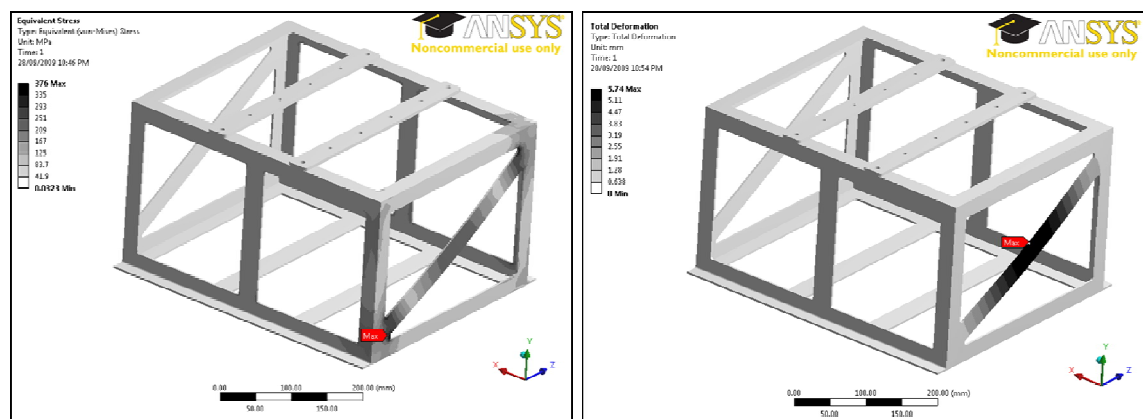


Figure 2.4.1-3: Left - rear impact von Mises equivalent stress contour plot and right - deflection contour plot.

The rear impact was simulated by the application of a 2500N force distributed across the rear facing face. It can be seen from figure 2.4.1-3 that the maximum stress and deflection occur in a similar manner to the side impact. The maximum von Mises equivalent stress of 376MPa occurs at the short radius corners and the maximum deflection of 5.8mm occurs at centre which is least supported and has the most flexibility.

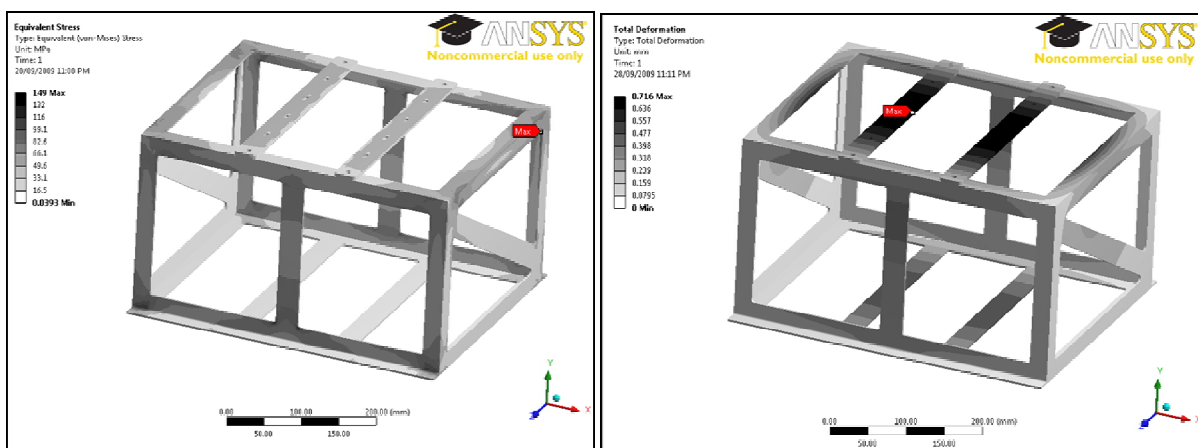


Figure 2.4.1-4: Left - vertical impact von Mises equivalent stress contour plot. Right - deflection contour plot.

The maximum vertical impact von Mises equivalent stress of 149MPa and maximum deflection of 0.8mm contour plots are shown in figures 2.4.1-4. It is evident from the low von-Mises equivalent stress that the structure is capable of a much larger vertical load due to the additional support at the base provided by the chassis.

Summarising the results:

Load Combination	Max. Equivalent Stress [MPa]	Max. Deflection [mm]	Percentage of Ultimate Strength
Side Impact (5kN)	344	4	78%
Rear Impact (2.5kN)	376	5.8	85%
Vertical Loading (5kN)	149	0.8	34%

Table 2.4.1-1: Summary of battery cage stress analysis.

The stress analysis demonstrates the optimisation of the battery cage such that all reasonable foreseeable loads will result in stresses below the 440MPa ultimate strength of the material. As these are not static loads expected during the service life of the cage,



the high stresses in the analysis as a percentage of ultimate strength shown in table 2.4.1-1 are considered acceptable. Based on this analysis, in the event of an accident the battery cage will need replacement because the stresses will exceed the 320MPa yield strength of the material and plastic deformation will result.

### 2.5 Manufacturing

Manufacturing was carried out by EV Works, a Perth company specialising electric car conversions. Flush welds were requested inside the cage to properly accommodate the batteries as per the design.



Figure 2.5-1: Left - manufactured battery cage; right – battery cage in its location behind the driver's seat.

The top bolts were countersunk to provide as close to flush as possible a face for the polycarbonate plate to seal against. The unit was sandblasted, primed and painted in black high gloss enamel lack to prevent corrosion and match the rest of the existing vehicle.

## 2.6 Evaluation & Future Work

The battery cage that was developed as a result of this analysis has satisfactorily met the requirements as stated in section 2.2: an optimised unit weighing 6kg that can house all the batteries and BMS units within a waterproof housing and resist minor side and rear impact.

This analysis is limited to the static loading on the battery cage. A further analysis would account for the dynamic effects of the vehicle moving up and down and the shift in weight during acceleration and braking. Proper guidelines as to the loading requirements would simplify the process and produce a more accurate result that could potentially reduce the weight of the battery cage. With some minor modifications to the chassis the connector, contactor and fuse could all be located in the same unit as the batteries to reduce the need for waterproofing additional components.

### **3. Wheel Hub Motor**

This section describes the requirements, design and evaluation of the wheel hub motor developed for the REV FSAE vehicle.

#### **3.1 Background**

A wheel hub motor is defined as drive mechanism that is integrated into the hub of the wheel, typically forming part of the unsprung mass of the vehicle. The use of an electric wheel hub motor could potentially eliminate the need for the petrol engine, gearbox or transmission and differential which reduces the weight and manufacturing costs of the drive assembly. The wheel hub motor can be more efficient than an inboard drive system as there are no mechanical losses through the gearbox, differential and CV joints (Carmody 2003). Each wheel can have by-wire control of drive, braking, suspension and steering. For the vehicle owner this translates to fewer components, reduced mechanical wear and service complexity.

Disadvantages of this drive mechanism include the increase in unsprung mass which results in wheel hop and reduces the responsiveness of the suspension and steering (Nagayo 2003). Three of the most popular systems are discussed: the Siemens VDO eCorner; Michelin Active Wheel and Protean Electric Hi-Pa Drive.

### 3.1.1 Siemens VDO eCorner

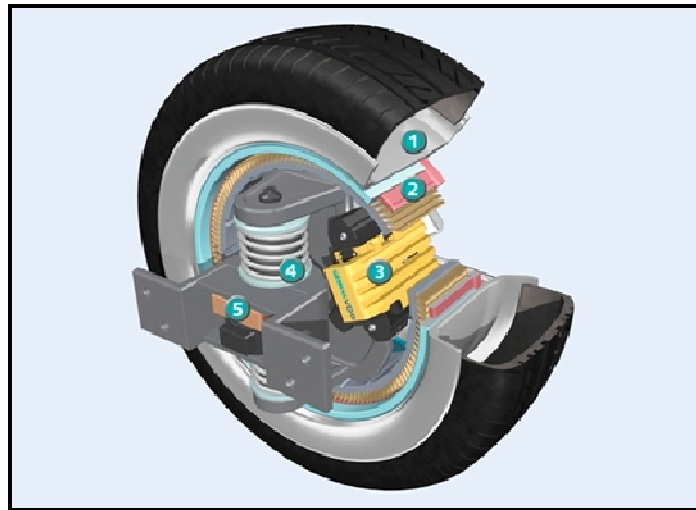


Figure 3.1.1-1: The rim of the wheel acts as the rotor and the internal hub is fixed as the stator as in the Siemens VDO eCorner concept (Siemens 2006).

The Siemens VDO eCorner wheel hub motor design integrates the drive train, steering, shock absorbers and brakes directly into the wheels. The developer claims that the uncooled wheel hub motor units could deliver up to 600Nm of torque to the wheels while the actively cooled could deliver up to 1000Nm of torque while still keeping the unsprung mass below 20% of the total wheel weight (Siemens 2006). For car owners this results in improved fuel economy, more safety and greater convenience. The eCorner is the most complete wheel hub motor, integrating the suspension and offering by-wire steering, giving automotive designers greater freedom and cabin space.

### 3.1.2 Michelin Active Wheel

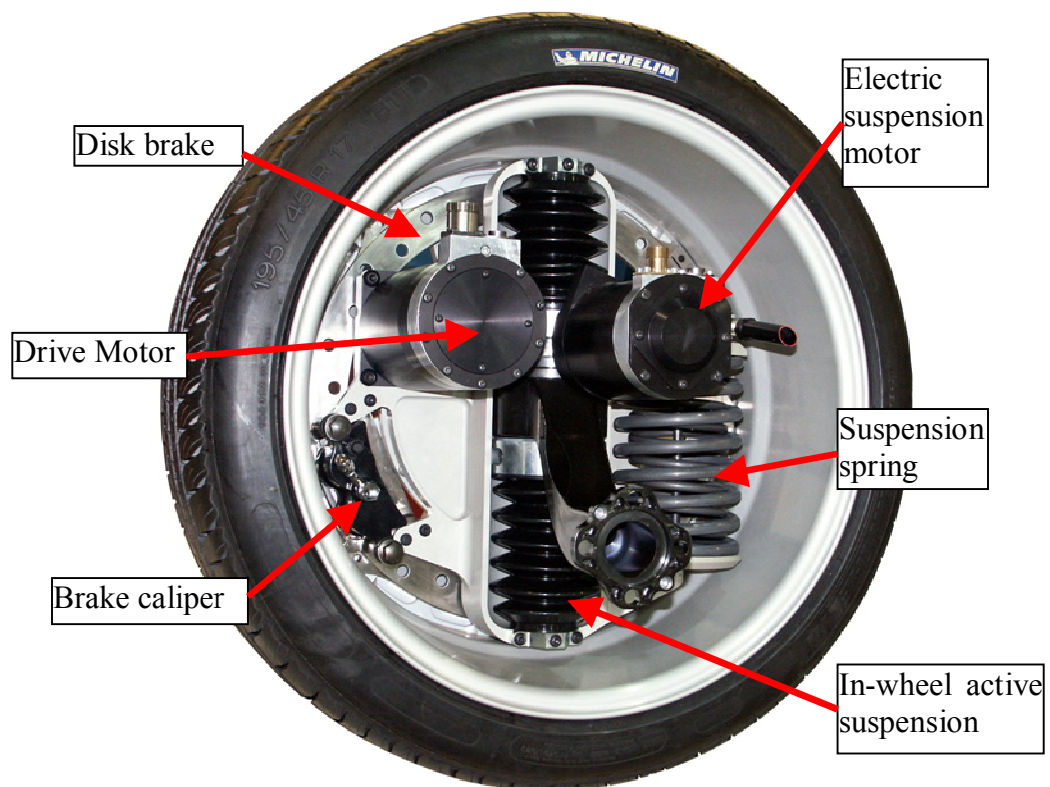


Figure 3.1.2-1: in-wheel motor – a separate electric motor drives the wheel rim as in the Michelin Active Wheel system (Michelin 2008).

The Michelin Active Wheel Motor weighs 42kg and includes a continuous 30kW rated water-cooled drive motor that drives a gear on the hub (Michelin 2008). A second electric motor operates the active suspension via a gear rack and pinion that replaces the normal hydraulic shock absorber. There is also a coil spring to hold the static load of the car and a small outer rotor disc brake. The wheel motor is attached to the vehicle chassis by a single lower control arm suspension arrangement. This type of system requires a mechanical friction brake for low speed braking as the regenerative abilities of electric motors are reduced at low speeds.

### 3.1.3 Hi-Pa Drive

Perhaps the most promising wheel hub technology is the Hi-Pa drive that contains the drive, brakes and electronic components into a weatherproof unit. It uses a water-cooled, 24 phase brushless DC pancake motor at up to 1800 RPM, driven by 120kW inverters which the manufacturers claim delivers 480A at 450V. The unit weighs 24kg and is supported by heavy-duty tapered roller bearings that can withstand the large radial loads sustained in a high performance vehicle (Boughtwood 2008).

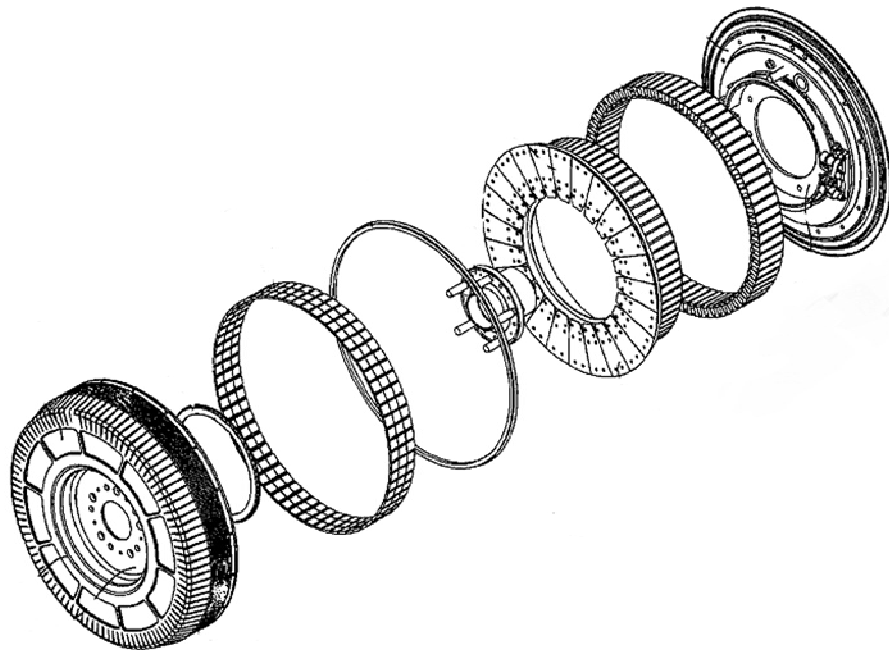


Figure 3.1.3-1: Protean Electric Hi-Pa Drive exploded view (Boughtwood 2008).

The supplier claims that regenerative braking is integrated into the motor, as well as the ability to hold the vehicle at a complete stop, eliminating the need for mechanical brakes. The suspension and steering are not integrated, so these wheel hub motors can be retrofitted to an existing vehicle. They offer the lowest weight and highest power density of all three concepts and will be the choice for the first mass produced high performance wheel hub motor driven vehicle – the Lightning GT (Lightning 2009).



### 3.2 REV FSAE Wheel Hub Motor

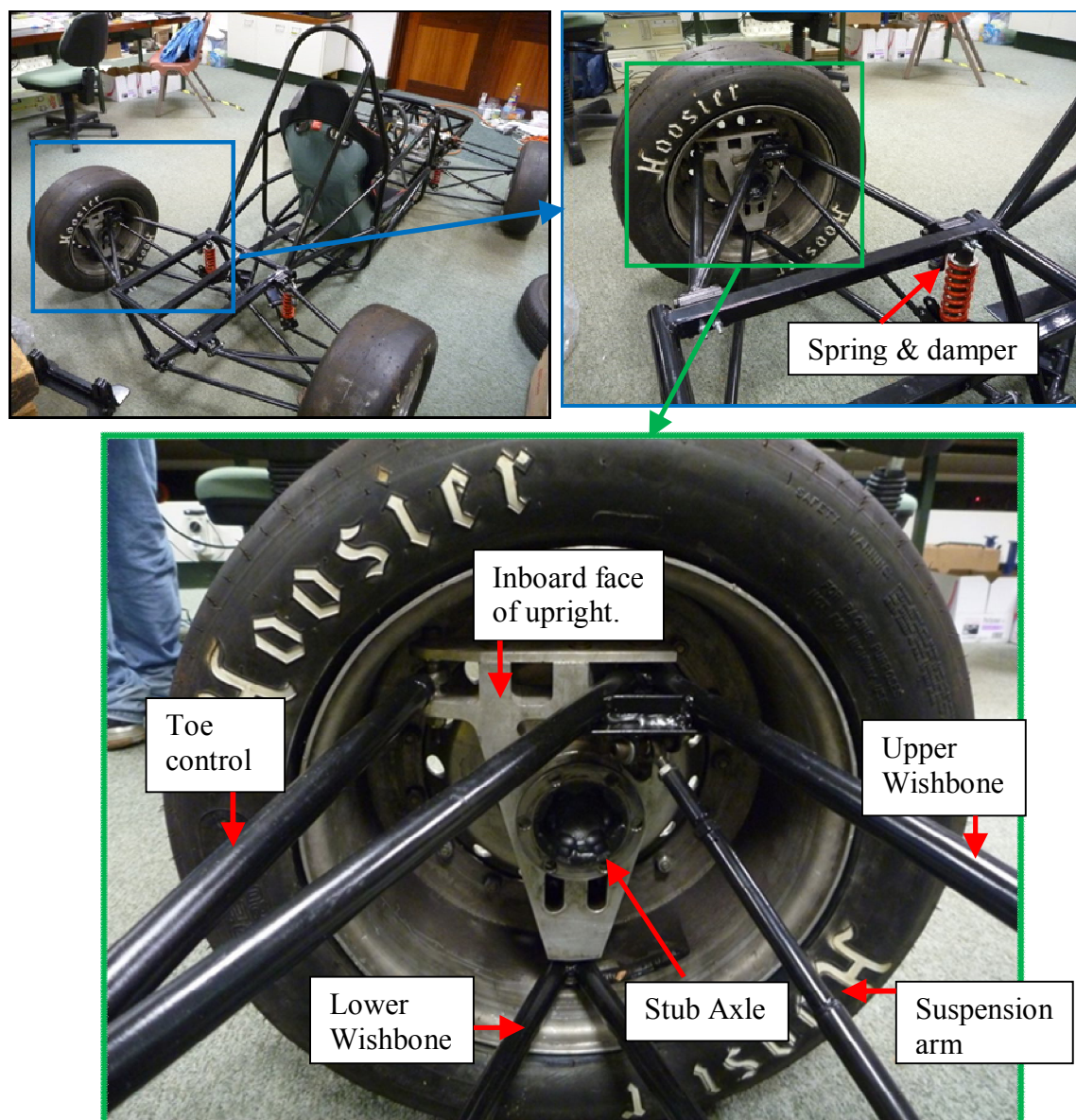


Figure 3.2-1: Rear left wheel of the REV SAE vehicle showing components referred to throughout the document.

The wheel hub motor method of driving the vehicle was initially imposed on the REV FSAE project. Inboard drive mechanisms connected to the wheel through a drive shaft were explicitly denied for 7 of the 8 month project duration and not investigated. As a result, the majority of time was spent sourcing a suitable motor, and designing a drive and packaging system because a retrofitted system had severe power handling limitations if weight was to be kept low, as required for a performance wheel hub motor system. The other option considered was the design of a completely new wheel hub

motor; however this was not financially possible and beyond the technical knowledge of the students. No budget was assigned for the REV FSAE team, nor was there a time frame defined in which the REV FSAE team could expect funding.

### 3.3 Requirements

As the project was first defined, there were several requirements expected during development and of the final mechanism as detailed below.

- **Drivable** - The vehicle *must be drivable* at the end of the 8 month project duration in order to generate sponsorship for the REV team.
- **Simplistic and low cost** – limited personnel, funds and time were available for the manufacture of any system.
- **Retrofit** – the drive mechanism must be attached to the existing upright to be classed as a wheel hub motor.
- **Light weight** – The wheel hub motor forms part of the unsprung mass of the vehicle which must be kept to a minimum.
- **Different motors** - The assembly must be able to take a variety of motors with varying power ratings and maximum RPM as larger motors were expected when funds became available.
- **Variable ratios for different motors** – higher powered motors with different and unknown characteristics were expected to be used at a later stage.
- **Performance** - Aim to at least match the performance of the 2001 petrol vehicle.

### 3.4 Motor Selection

An investigation was carried out with the electrical team to determine the maximum power and torque required to drive the vehicle and attempt to match the performance of the 2001 UWAM FSAE vehicle setup. This had to be matched with the 48V maximum safe voltage allowed by the Hybrid competition rules, as well as the maximum current that can be drawn from the battery pack.



Using an arbitrary acceleration of 0 to 100m in 5 seconds, approximate mass of the vehicle of 250kg, the power required to accelerate the vehicle is calculated below where m is mass, v is velocity, t is time:

$$E = \frac{mv^2}{2} \quad \text{Eq: 3.4-1}$$

$$P = \frac{mv^2}{2t} \quad \text{Eq: 3.4-2}$$

$$P = \frac{250 \times \left(\frac{100}{5}\right)^2}{2 \times 5} = 19290W \quad \text{Eq: 3.4-3}$$

A desired maximum vehicle speed of 120kmh<sup>-1</sup> was used with the maximum allowable angular velocity of the electric motors expected at 6000 RPM to determine that the required reduction ratio from motor to wheel was in the order of 5:1.

A simplistic calculation was also performed to determine the maximum torque required to break traction of the vehicle at the rear wheels in a straight line during high acceleration. Based on the forecasted weight of the vehicle and a range of coefficients of friction depending on tyre and road condition, the torque range is 100 – 150Nm.

A cost benefit analysis was then conducted to find a motor with an approximate maximum power rating of 10KW per wheel and also matching the requirements used to define the project.

Preliminary findings:

Ruled out direct drive hub motors such as the Hi-Pa where the wheel itself is the rotor as it is:

- Prohibitively expensive (over A\$20,000 per wheel).
- Of unknown availability and lead-time.

Ruled out hub motors used in electric scooters because:

- Cannot be found above 3kW.
- Not designed for 4 wheeled vehicles so the shaft is too weak to be held on a single side only.
- Poor brakes.

No high performance AC induction motors were identified with the required size and power.

 <p>Mars PMSM (Mars 2007)</p>	 <p>AGNI/Lynch 95 (Agni Motors 2009)</p>	 <p>ADC 140-07-4001 (EV Parts 2009)</p>
 <p>Perm PMS100 (Perm Motor 2009)</p>	 <p>HXT 80-100-B (Hobby King 2009)</p>	 <p>Plettenberg Predator (Plettenberg 2005)</p>

Figure 3.4-1: Selection of motors considered as potential candidates.



Motor	Technology	Power	Efficiency	Weight	Dimensions	Cost	Advantages	Disadvantages
Mars PMSM	Axial BLDC	5kW cont 15kW peak	90%	10kg	ø250 x 150	~\$700	Sensored*, good continuous power	Large size and weight
AGNI/Lynch 95 series	Axialbrushed DC	9.6kW cont 29kW peak	93%	11kg	ø210 x 150	~\$1500	Very high power	Large size and weight, poor regen with brushed DC motors, expensive
Advanced DC 140-07-4001	Series DC	1.6kW cont 9.9kW peak	75%	13kg	ø140 x 210	~\$1000	Robust	Poor power density, low efficiency, regen not possible
Perm PMS100	Axial BLDC	3.0kW cont	91%	5.6kg	ø190 x 120	~\$1500	Quality, industrial design, sensed*	High price, modest power density
HXT 80-100-B	BLDC Outrunner	6kW Peak**	91%	1.5kg	ø100 x 100	\$275	Low price, very high power density	Sensorless*, external cooling may be required
Plettenberg Predator 37	BLDC Outrunner	15kW peak**	88%	1.9kg	ø100 x 75	\$1500	Extremely high power density	Sensorless*, external cooling may be required, expensive

\* Brushless motors may be sensed or sensorless, referring to sensing of armature rotation. With sensorless brushless motors, the motor controller relies on back EMF for rotational position sensing which only works while the motor is moving, so they have poor starting torque and usually no regenerative braking offered by the controller. It may be necessary to add a rotation sensor and use with a more advanced controller supporting sensed motors.\*\* With sufficient forced convection cooling which may be necessary to add.

Table 3.4-1: Specifications of potential electric motors considered for the hub motor design.

The limited budget and space constraints lead to the purchase of a single HXT 80: a brushless DC outrunner motor typically used in large-scale model aircraft to drive the propeller. In concept they were ideal as the vehicle required peak power for only short bursts during acceleration and autocross, yet they remained light weight enough to have the least impact on unsprung weight and vehicle dynamics.

This type of motor offered a comparatively high power density and low weight which were identified early in the project as dominating factors on the performance of the design and vehicle dynamics. As HXT motor only offered an inadequate 6kW peak power, the intention was to upgrade to the Plettenberg Predator when funds became available and issues with this type of motor were identified and resolved in testing with the HXT 80.

The torque rating of the motors is not given, but it is possible to work backwards from the quoted peak power using the fact that power is angular velocity multiplied by torque. The torque is found to be approximately 10Nm for the smaller HXT motors, and 20Nm for the larger Plettenberg Predator model. Using a 5:1 reduction ratio, the larger Plettenberg would only *just* meet the requirements to break traction in a straight line during high acceleration.

### 3.5 BLDC Outrunner Issues

#### *3.5.1 Limited Start-up Torque*

Any design produced with this type of motor would have to account for limited start-up torque. The intended application of the motor was to run propeller blades which have a small opposing torque at start-up. In their intended application, the motor starts by delivering a large surge of current to start the rotor spinning, then use the back EMF to sense the position of the rotor.

In the REV FSAE vehicle, the motor needs to start with a large opposing torque at it would be connected to the wheel and have to propel the vehicle in order to start the rotor spinning and generate the required back EMF. To operate in the same way with a large current would overheat and damage the motor as it would have to be sustained until the motor reached the required RPM to generate the back EMF and sense the rotor

position. To remedy this issue, the HXT 80 motor purchased was used for the development and testing of a Hall Effect sensor system to sense the position of the rotor instead of using motor back EMF. A Plettenberg Predator motor would be purchased once the Hall Effect sensor system was proven on the HXT because both motors operate by sensing back EMF.

### *3.5.2 Overheating*

The quoted specifications of the HXT and Plettenberg motors is the *peak* power and torque rating. This value is defined by the manufacturer in the context of its intended application in model aircraft where the opposing shaft torque is only due to the blade inertia and wind resistance, and there is ample airflow to cool the motors during high current demand. The Plettenberg manufacturer documentation explicitly states that the use of their electric motors in vehicles voids warranty as there is the potential to overheat.

Additionally, the bearings in the motors were not designed to take a large lateral load, or to withstand vibration. This was an issue in the design because the motor formed part of the unsprung mass where the only damping and shock absorption was provided by the vehicle tyre.

However, these motors were the *only* accessible motors rated at or below the maximum safe voltage that could be packaged into the wheel of the vehicle and kept the unsprung mass low. The other options are simply too large, too heavy or too expensive for a wheel hub motor.

### *3.5.3 Inboard Appeal*

The results of the required power and torque calculations; the cost-benefit analysis and the limitations and risk of the only feasible HXT and Plettenberg motors were made clear to the REV academic leadership early in the development phase. A concise, logical case was presented to delay the use of a wheel hub motor concept to a later version of the vehicle when sufficient funds and research time would be available. It was suggested by the REV FSAE student team to design an inboard solution with motors mounted to the chassis and connected to the wheel through a pair of CV joints and modified axle for the first electric iteration of the vehicle. This method would not be bound by the same weight and packaging limitations as the wheel hub outboard design,

and could be quickly produced because standard motors and controllers existed for the intended application.

The author's suggested inboard drive mechanism was rejected by REV academic leadership. As a result, the wheel hub motor concept continued, attempting to deliver a low cost wheel hub motor design capable of withstanding the required power and torque while being adjustable for both multiple and different motors; minimising weight, vibration and overheating.

### 3.6 Reduction Mechanism

Four different drive mechanism types were investigated for the wheel hub motors to step down the required 5:1 ratio from the electric motor to the wheel: pulley, chain, spur and planetary gear drive. In addition to meeting the minimum requirements already described, the following criteria were also used to scrutinise potential designs.

- **Safety** – minimising exposed rotating components and the risk of electrocution.
- **Manufacturability** – reducing complex geometry and the need for dangerous and expensive manufacturing techniques.
- **Cost** – Reducing part count and using industry standard components that are easily sourced.
- **Weight** – Using light weight components, preferably aluminium alloy.
- **Vehicle dynamics** – Impact on weight distribution and effect on wheel position.
- **Serviceability** – Consider how the design would be assembled; access to and the replacement of components.
- **Performance** – meeting the stress analysis requirements and reducing mechanical losses. Consider the potential for failure and breakdown.

#### *3.6.1 Chain and Sprocket*

The chain and sprocket drive system was investigated for transmitting power from the electric motor to the axle of the wheel. The practical experiences of the UWA Motorsport team in combination with a literature review lead to the following conclusions. The chain drive system was found to have many advantages including:

- Low price and readily available as industry standard components.

- Positive meshing for more compact reduction than belts for the same ratio.

However it was rejected as a drive mechanism for the following reasons:

- The chain drive needs regular cleaning and greasing maintenance.
- The chain and sprocket need shielding for safety and to also to contain any grease flicked from the chain.
- The chain length needed to be precise and a tensioner used or the chain will run with slack and increase wear.
- Pulley and belt drives with similar power and torque handling capacity were available (Gates 2009c).

### 3.6.2 Spur Gears

A pair of spur gear was another method considered to transmit power by connecting the pinion gear to the motor shaft and the larger gear to the wheel axle, in the required 5:1 ratio. The setup was investigated with the pinion gear both inside and outside the axially mounted stub axle gear as shown in figure 3.6.2-1 depending on the size of the motor used and the space constraints.

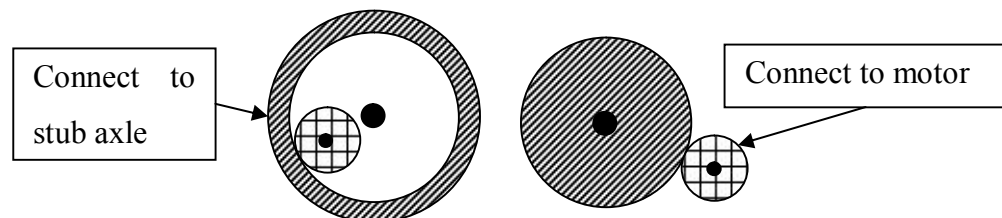


Figure 3.6.2-1: Potential spur gear assembly.

This type of system offered a more compact solution than pulley and chain drives; however it was rejected because a pre-manufactured system could not be sourced in the required ratios at a reasonable price and would have resulted in a system that weighed too much or was not rated for the required torque.

Manufacturing a set of gears specifically for the project was expensive and would also require an enclosure to contain lubricant and shield the gears for safety reasons. Although this may seem a limited treatment of the option, the investigation was enough to determine that spur gears were not a viable option and that other more suitable methods existed.

### 3.6.3 Planetary Gears

In a planetary gear setup, a central sun gear is surrounded by three or more planetary gears mounted to a carrier, which are also coupled to an outer ring gear as shown in figure 3.6.3-1.

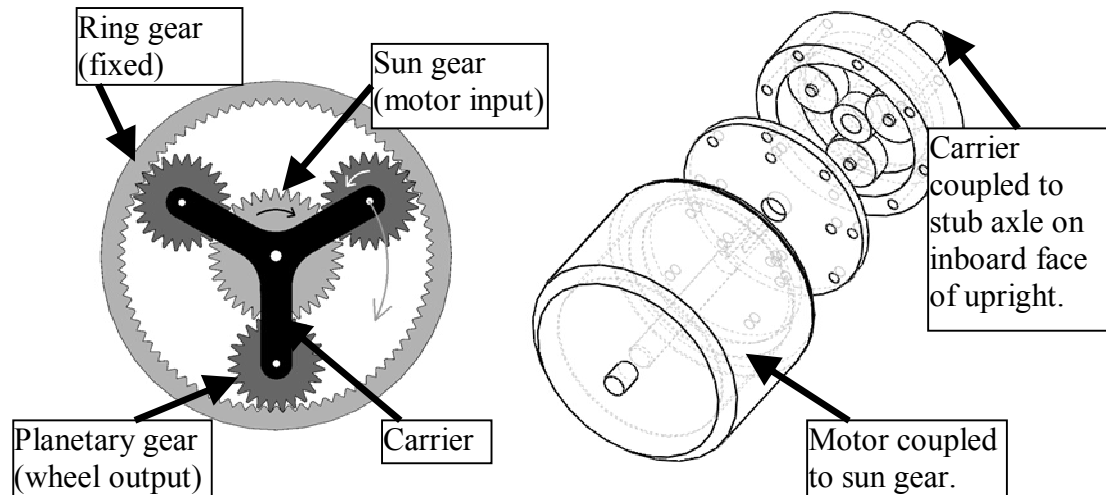


Figure 3.6.3-1: Planetary gear train.

In the trial setup, the ring gear is held stationary to the upright; the motor shaft is coupled to the sun input gear and the planetary gear set carrier is connected to the wheel axle as the output. The planetary gear set has the following advantages:

- High power and torque density over a spur gear setup due to multiple planet gears.
- High power transmission efficiency (Cho 2006).
- Compact and axial mounting results in greater stability and rotational stiffness (Cho 2006)
- Large and various reduction ratios possible depending which gear is kept stationary and which is used as the input.



Both the manufacture of a planetary system and the purchase of an already built unit were investigated, but the setup was eventually rejected for the following practical reasons:

- Axially mounting the planetary gear box and a motor required a redesign of the rear suspension for which there was limited experience in the REV FSAE team, no allocated workshop time and very limited funds available.

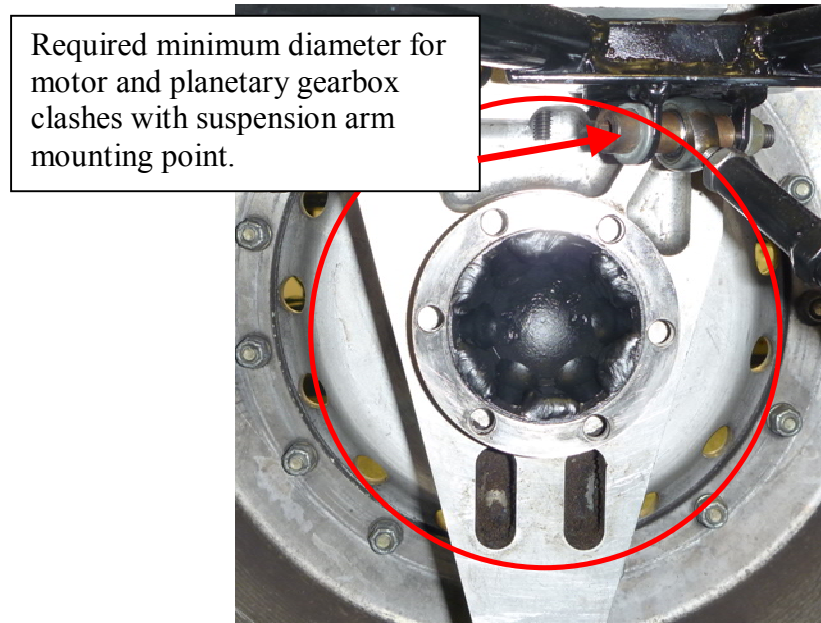


Figure 3.6.3-2: suspension arm in the way of axial mounting of motor and gearbox on the inboard face of the upright.

- Small planetary gear boxes are difficult and expensive to source in the required ratios.
- Using stock components such as the gear sets from small automatic transmissions or starter motors would have been ideal however it required the manufacture of a sealed unit with oil or grease, for which there was no funds available.

### *3.6.4 Synchronous Pulley and Belt*

The synchronous (also called toothed, timing or cog) pulley and belt system held the most promise during the preliminary research phase with the following advantages.

- It was low cost, easily accessible with standard components common to various industries.
- It tolerated minor misalignment between the input and output pulleys which was advantageous when designing to control vibration (Gates 2009d).
- Ideal tension is the lowest required to properly seat the teeth of the belt in the pulley.
- Belts were available that could match chains for the same thickness due to the curvilinear toothed profile of the belt and pulley (Gates 2009c).

Synchronous belts were less tolerant than V-belt drives to high shock loading and required more accurate alignment to prevent belt damage (Gates 2009d). However the synchronous belt was chosen over V-belt because it required less tension to operate, and was a more compact solution.

Packaging the pulleys and motors was difficult due to the required belt wrap around the pulleys for the expected power and torque, but still conceivable. As the most financially feasible option, the pulley system was chosen as the drive system to investigate to completion using the Rudimentary Design Process (Wright 2000).

### 3.7 Rudimentary Design Process

The six stages of the design process summarised below were followed through to their eventual conclusion until a design was achieved.

1. Problem statement - Ideally this design process would have been followed from the beginning of the project when designing a drive mechanism, but the wheel hub motor drive concept was artificially imposed as the only allowable drive system.
2. Creativity – non-critical brainstorming to explore and develop as many design candidates as possible.

3. Problem Completion – application of constraints and criteria defined in section 3.3 to the ideas generated during brainstorming.
4. Practicalisation – refining the concepts that successfully met the constraints during problem completion.
5. Evaluation – the degree of importance of each criterion is graded, and the potential solutions are evaluated against the graded criterion.
6. Communication – Designs are refined and visualised, the cost of each are investigated.

An abundance of potential solutions were hand sketched and modelled in Solidworks to check packaging, however only the pulley designs are presented in detail for the sake of brevity as they were found to be the most suitable at the conclusion of the Rudimentary Design Process. The pulley drive solutions that reached the practicalisation stage are presented below with a discussion of their development, refinement and evaluation.

#### *3.7.1 Design Development*

The initial and most simplistic solution was to mount the motor to the side of the upright and run a single stage pulley on the shaft of the motor to a larger pulley mounted to the stub axle to deliver the required 5:1 reduction ratio. It was quickly realised that due to the fixed motor dimensions, that this could not be packaged into the rim of the wheel without the pulleys clashing. The smallest driving pulley that could be used was 40mm so the required driven pulley would be 200mm due to the ratio, which would clash with the suspension so a two stage reduction was developed. This method reduced the size of the pulleys by adding an additional stage of reduction, but would introduce additional parts, complexity and expense.

An additional issue was the depth of the motor at over 100mm: any arrangement required the motor to protrude beyond the upright which was only 50mm deep. This would introduce large bending moments to both the motor shaft and the stub axle, or increase the track width of the vehicle which was highly undesirable.

#### *3.7.2 Two Stage Phase 1*

The first design was a naive attempt to satisfy all the design criteria by being fully adjustable and integrating a jaw coupling in case of failure as well as a small fan for

cooling, all shown in figure 3.7.2-1. The pulley was mounted with its own support that would take the belt tension to preserve the motor bearings.

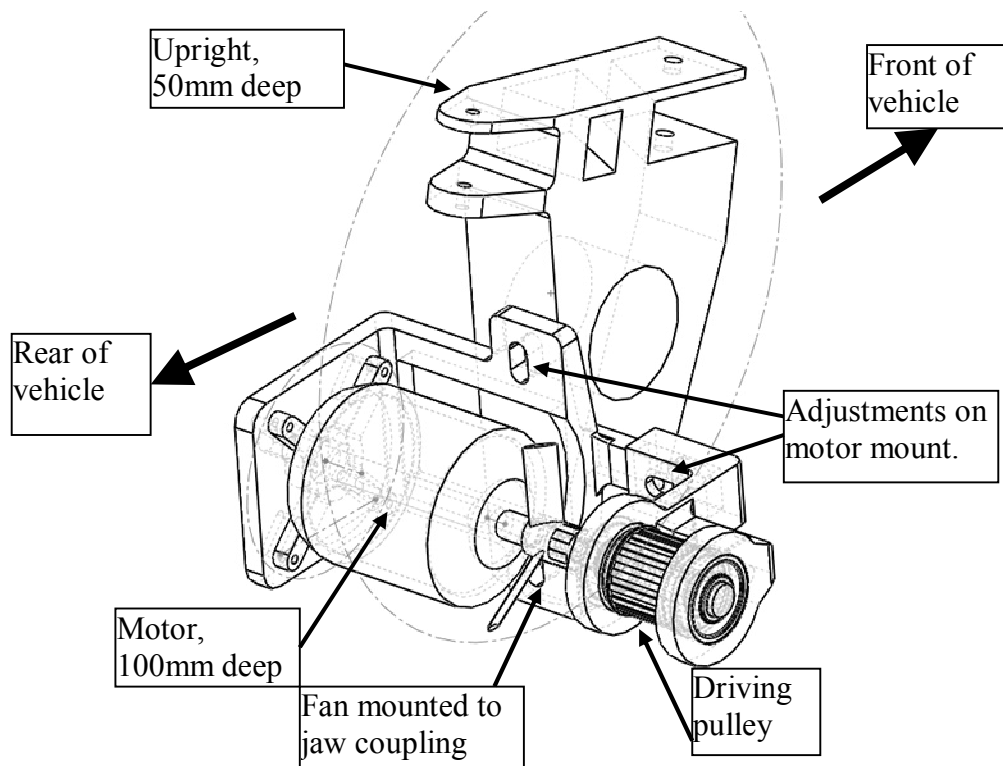


Figure 3.7.2-1: Ambitious but impractical design shown for the left rear wheel hub. The wheel, stub axle and driven pulley are not shown.

The arrangement in figure 3.7.2-1 was not suitable primarily due to the large bending moment applied to the motor mount by the belt tension acting on the driving pulley. It became evident that the attempt to satisfy all the design criteria resulted in a heavy and complex supporting structure. The requirements had to be refined and risks taken in order to simplify the design, so the integration of the failure coupling and cooling was removed.

### 3.7.3 Two Stage Phase 2

Investigation of the available pulleys for the required power and torque rating showed that the smallest available pulley was in the 40mm range in the required 25mm belt width (Gates 2009e). For the desired 5:1 reduction ratio, this would require a 200mm driven pulley which would clash with the suspension and wishbones. A two stage reduction was developed and shown in figure 3.7.3-1, and the assembly pushed further away from the vehicle to reduce the moment applied to the supporting structure at the expense of increasing the wheel track width.

The simple calculation for the two stage reduction ratio is shown here where R is the radius of the pulley (Waldron 2004).

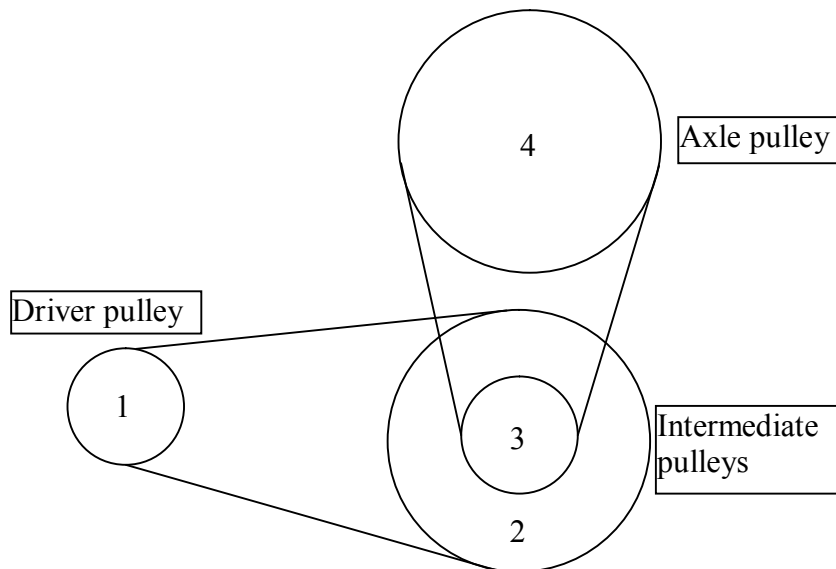


Figure 3.7.3-1: Calculation of reduction ratio using pulleys.

$$\text{Reduction Ratio} = \frac{R_2 \cdot R_4}{R_1 \cdot R_3} \quad \text{Eq:3.7.3-1}$$

Attempts were made to keep pulleys 1 and 3 of the same diameter, as well as 2 and 4 so that they could be interchanged and fewer part types sourced.

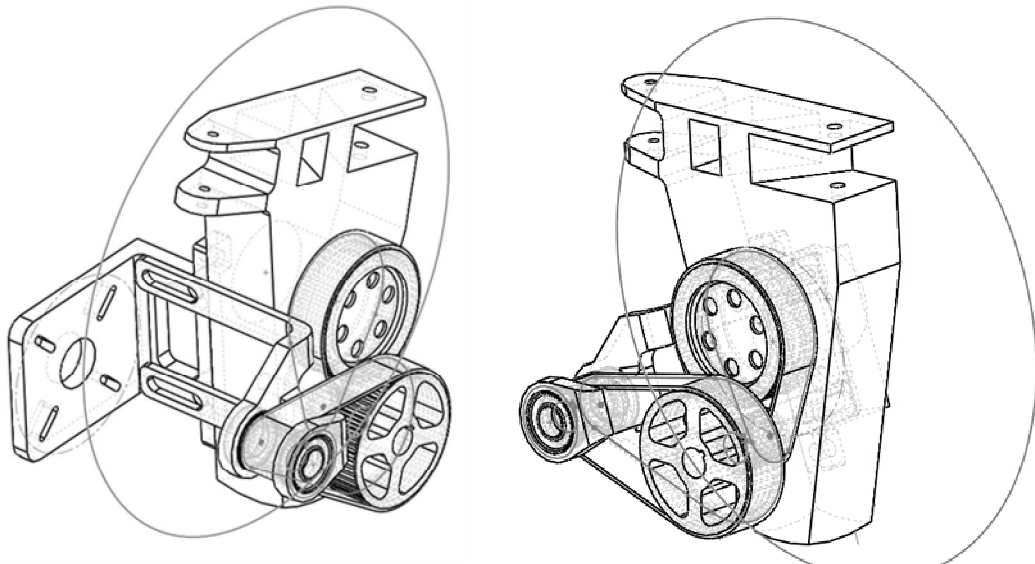


Figure 3.7.3-2: Introduce two stage pulley system – belt tension operates further from face of upright so introduces larger bending moment to motor mounting structure.

This system used smaller pulleys that could be found in the same pitch, but still applied a large bending moment to the small pulley support which would require significant strengthening and increased mass. This could be reduced by moving the motor towards the wheel, but this in turn will offset the wheel from the upright and increase the rear wheel track width.

### 3.7.4 Two Stage Phase 3

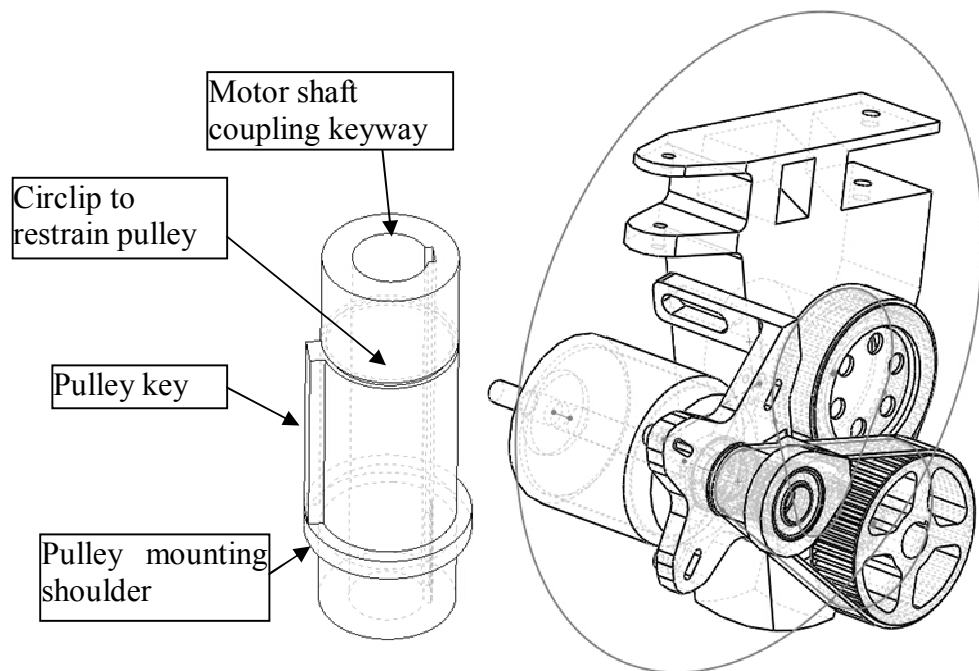


Figure 3.7.4-1: Optimization of the two stage design to reduce weight and the bending moment on the motor bearings.

The two stage design was refined by integrating the motor mounting plate with the pulley support structure. The motor coupled on its reverse side next to its mounting point rather than the propeller end. This reduced the applied bending moment to the motor, saved on material and reduced the number of components. The shaft shown in figure 3.7.4-1 was developed so that the motor shaft coupled directly into the pulley shaft and conserved space.

### 3.7.5 Two Stage Phase 4

Further refinements were made to the two stage design with the addition of a sleeve rotating over a shaft through two needle bearings. This was required to couple the intermediate pulleys to rotate with the same angular velocity through a key in the sleeve. However this sleeve is a minimum diameter of 30mm which increases the minimum diameter of the small intermediate pulley, hence the other pulleys need to be larger as well to achieve the required reduction ratio as per equation 3.7.3-1.

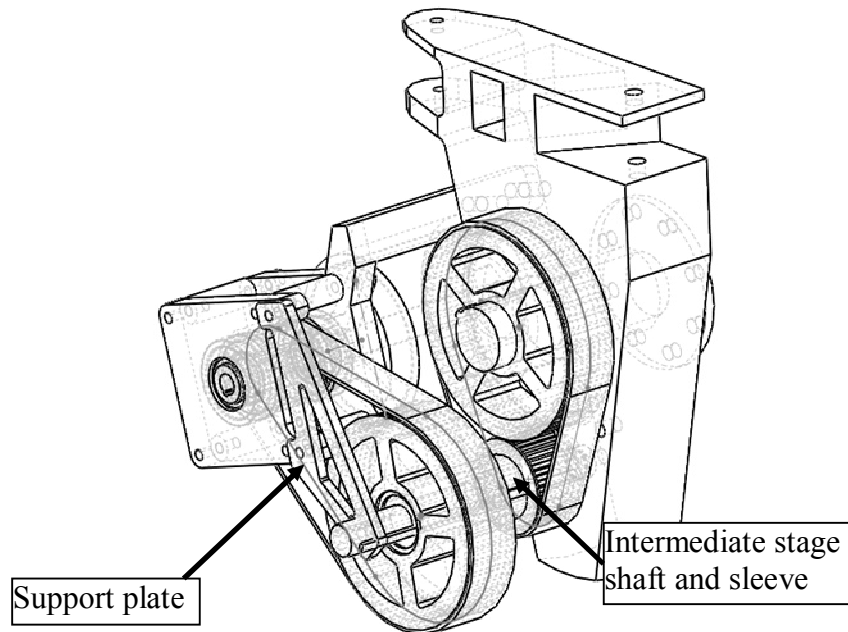


Figure 3.7.5-1: Addition of support plate and intermediate shaft and

Analysis of this shaft showed that it would have to be at least 15mm thick to take the applied bending moment and not deflect significantly enough to affect pulley alignment performance as per supplier specifications (Gates 2009a). In addition, a support plate is added to prevent deflection of the intermediate shaft.

#### 3.7.6 Two Stage Phase 5

Stress analysis showed that there is not enough material on the upright to bolt through for the intermediate shaft as used in design 4, due to a clash with a wishbone bolt through the base of the upright, so an alternative solution was found by using a bearing mounted to the side of the upright to support the intermediate shaft as shown in figure 3.7.6-1. This setup eliminated the need for a sleeve to mount the intermediate pulleys so their minimum diameter can be reduced to save weight and space. The support bracket across the front of the pulleys was combined to a single piece with the driven pulley support to reduce parts and increase its strength.



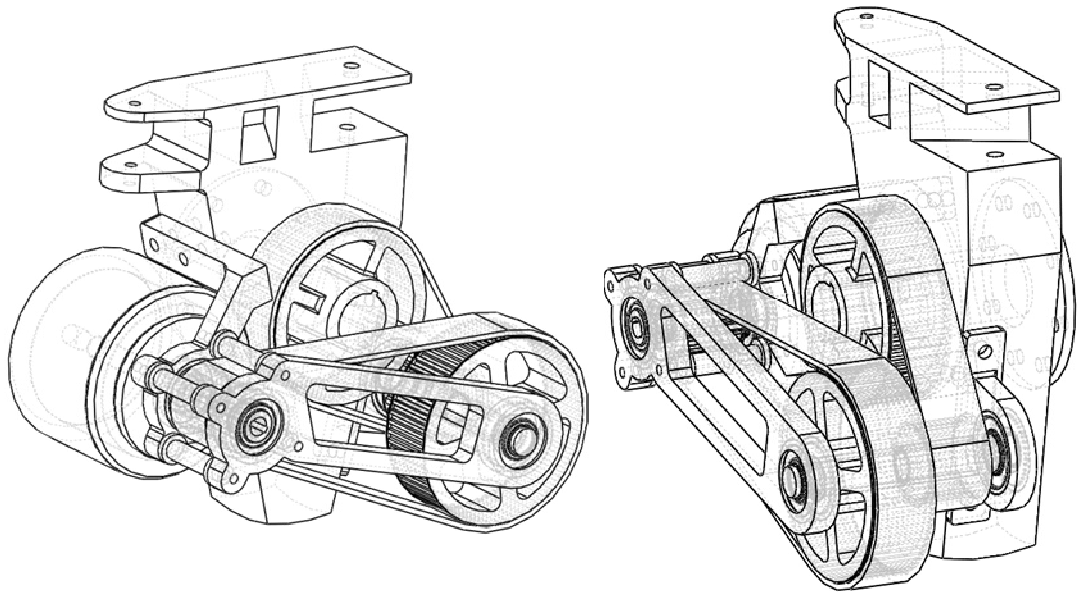


Figure 3.7.6-1: Left and right side of the final two stage.

The results of the stress analysis were used to optimise material distribution by increasing the thickness of the motor support bracket to withstand the weight of the motor during vibration and the stresses induced in the support due to the applied torque during acceleration and braking. The assembly in figure 3.7.6-1 was completed with appropriately placed keyways, shoulders, grub screws and circlips to locate and hold the two shafts and bearing couples in place. The assembly was designed so that no modifications are required to apply the concept to both left and right wheels. An exploded view of the assembly is available in appendix C.

### 3.8 Two Stage Stress Analysis

The stress analysis model of the final two stage reduction pulley wheel hub motor required simplification to reduce the number of parts that would have otherwise required user input to define relationships in the analysis. Additionally, roller bearings and friction contact between parts required far more processing time so the analysis was reduced to a simple static, bonded structure as shown in figure 3.8-1.

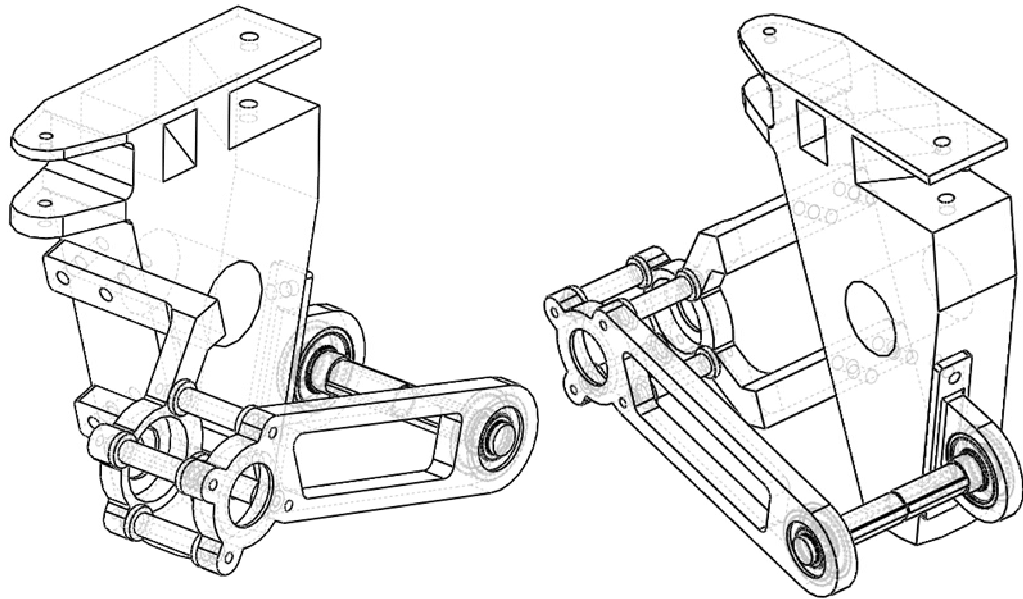


Figure 3.8-1: Simplified structure reduced stress analysis processing time.

Rather than modelling each component and relationship, the analysis was performed on the simplified structure with the application of a large safety margin. The material used for the analysis was 6061 Aluminium alloy with a yield strength of 276MPa (Alcoa 2006) which is easily machined.

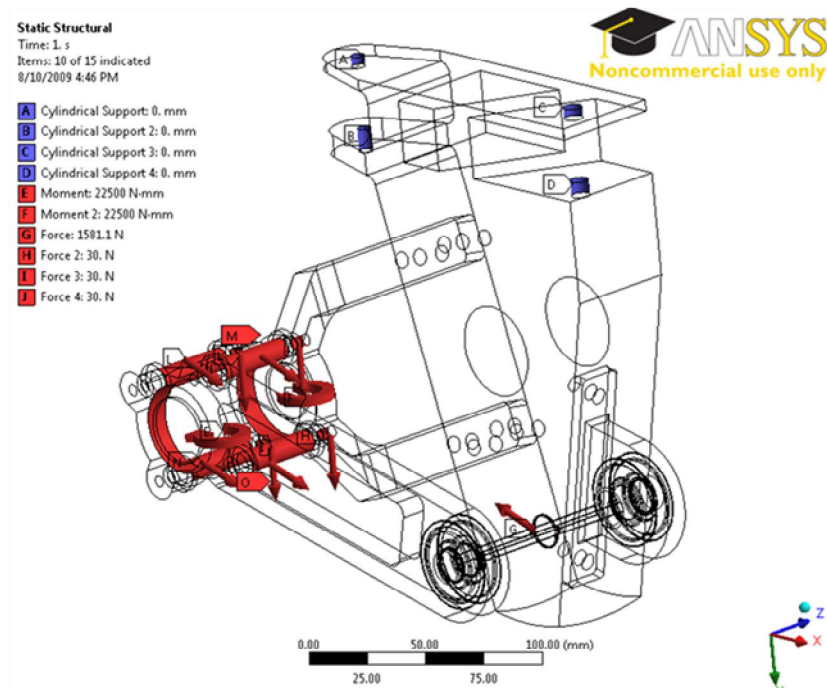


Figure 3.8-2: Supports and applied loads.

Loading and supports are shown in figure 3.8-2 and have been applied as follows:

- (G) - The maximum recommended load of the Gates belt at 1500N (Gates 2009d) has been applied to the intermediate shaft.
- (A,B,C & D) - The top and bottom bolts supporting the upright have been approximated by cylindrical supports
- (E & F) - The tension on the motor pulley applied to the bearing seats as a bending moment equal to 22.5Nm to each face by converting the pulley tension to an applied moment.
- (H, I, J & K) - Triple the weight of the motors has been used and distributed across the four motor bolt holes to account for the weight and any dynamic amplification of the force during wheel hop.

This analysis assumed that the bolts will not fail and that the bolt force is high enough that the frictional interface between components could be approximated by a bonded surface. In reality there would be additional support provided by the shaft and bearings to which the motor attaches, however they have been omitted for simplicity.

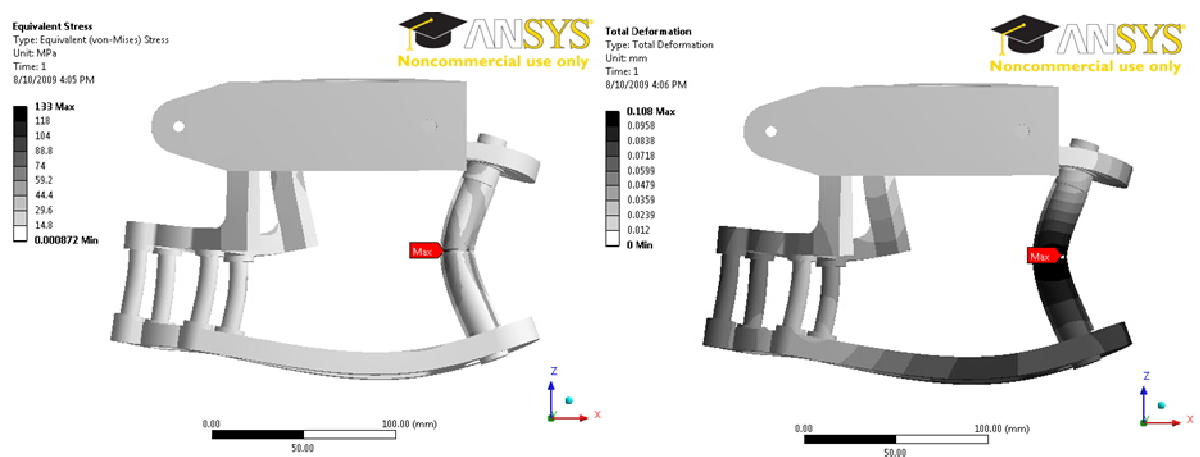


Figure 3.8-3: Top view of maximum von-Mises equivalent stress (left) and Maximum total displacement (right) with an exaggerated scale for clarity.

It can be seen that even with the conservative applied loads, the maximum stress of 133MPa is below the yield strength of the material at 276MPa and the maximum deflection of the shaft is only 0.11mm which would not affect the pulley alignment and performance as per the pulley supplier installation and maintenance guide (Gates 2009a).

### 3.9 Two Stage Design Evaluation

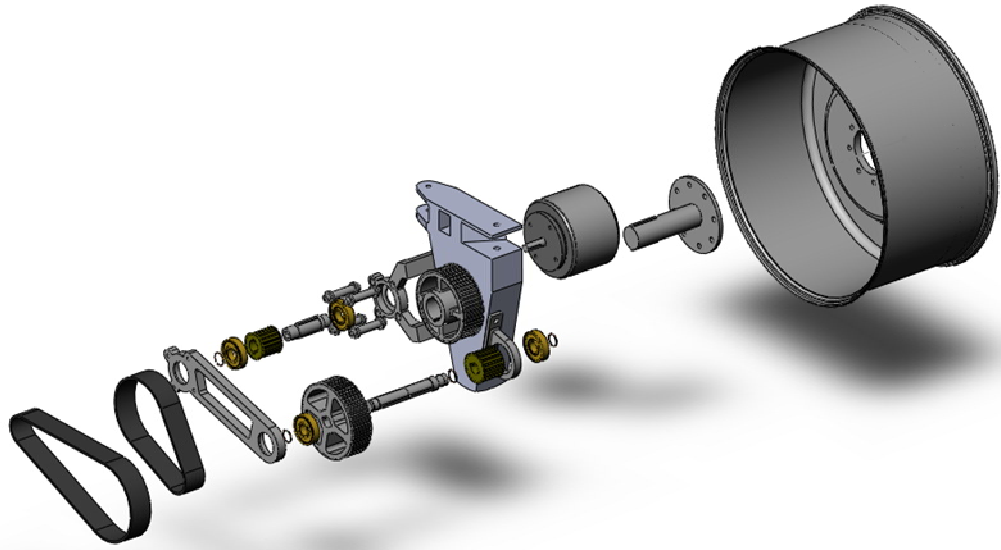


Figure 3.9-1: Exploded view of the final two stage assembly.

This design only partially meets the design requirements used to define the process in section 3.3. It is a stress analysed, retrofitted, low cost assembly attempting to use industry sourced components. The geometry is simple and no expensive manufacturing techniques are required. Physically assembling it is straightforward and all components are easily accessed for service and replacement. The assembly is kept light and the track width of the car is not modified. However there are a large number of parts used as shown in the exploded view in figure 3.9-1 and the design does not address the critical failure modes of the motors: overheating and vibration.

### 3.10 Single Stage Design

A single stage pulley reduction system was also investigated as part of the Rudimentary Design Process as it was considered a feasible option for a wheel hub motor. The two stage design mounted the drive on the inside of the upright that faces the vehicle. In that design there was limited room due to the wishbones and suspension arms so a single stage was not possible. However it is entirely feasible when the larger driven pulley is mounted between the wheel and the upright as shown in figure 3.10-1.

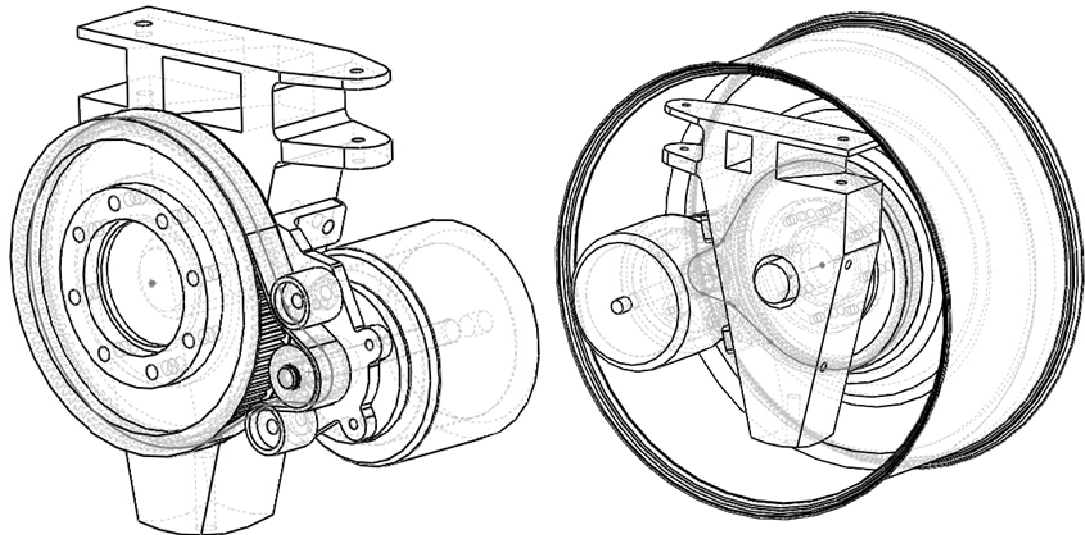


Figure 3.10-1: Single stage with the large axle pulley mounted between the wheel rim and upright.

This arrangement had many advantages over a two stage system due to its simplicity:

- Fewer parts
- Lower weight
- Easier to assemble
- Accepted various motor lengths

However there were also drawbacks:

- Significantly reduced belt life because idlers wrap across the back of the belt at a small radius to give required belt wrap around driving pulley (Gates 2009d).
- Increased the offset of the wheel by an additional 10mm to accommodate the 25mm width pulley and belt required to deliver the power and torque.
- Pulley access required wheel removal.
- The driving pulley had to be kept very small at 30mm diameter, and the motor shaft had to mount directly into the pulley. This meant that all belt tension was applied to the motor bearing as a sustained moment, which it was not designed to withstand (Plettenberg 2005).

#### *3.10.1 Single Stage Stress Analysis*

The stress analysis of the system was simplified as only the motor mounting plate component was required as shown in figure 3.10.1-1.

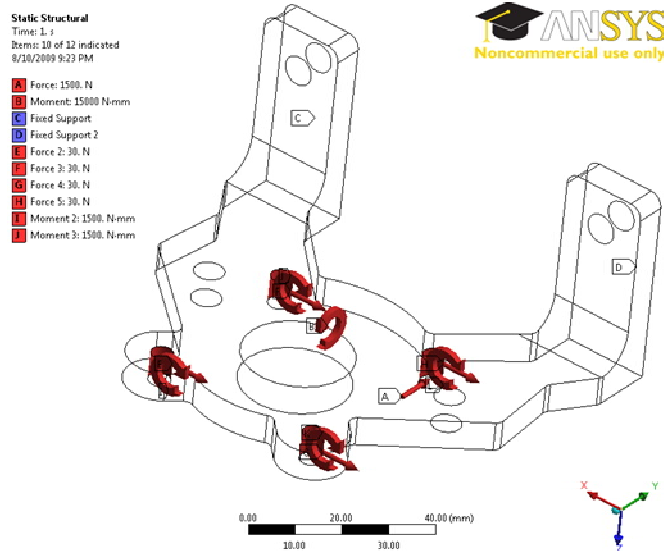


Figure 3.10.1-1: Applied loads and fixed supports to motor mounting plate.

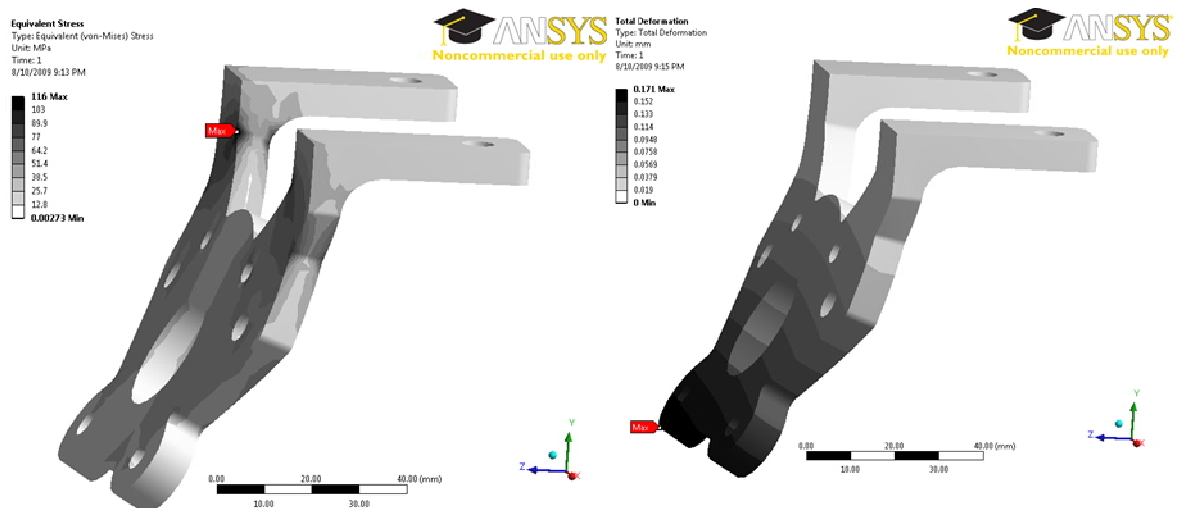


Figure 3.10.1-2: Left - von-Mises equivalent stress and right - total deflection for the motor mounting plate.

A force of 1500N has been used to simulate the belt tension. The motor weight force and resulting bending moment have also been applied, all as shown in figure 3.10.1-1. It can be seen that the maximum stress of 116MPa occurs at the elbow due to the bending moment caused by the belt tension. This is well below the 276MPa yield strength of the 6061 Aluminium alloy construction material.

### 3.11 Future Work

With the required financial support, the modifications to the suspension and a purpose designed and built upright, the use of a planetary gearbox would present the most power and torque handling density in a light weight, compact design. The current hollow UWAM '09 vehicle uprights should be redesigned to include a planetary gear set from a small automatic vehicle transmission such as that shown in figure 3.11-1. This would be a high power density, sealed unit with a passive oil supply. This could couple to a brushless DC pancake plate motor which offers a flat profile with the highest torque rating. Additionally, active cooling should be investigated as the torque is proportional to current, and the power handling is partly limited by the rate at which heat can be dissipated from the motor.

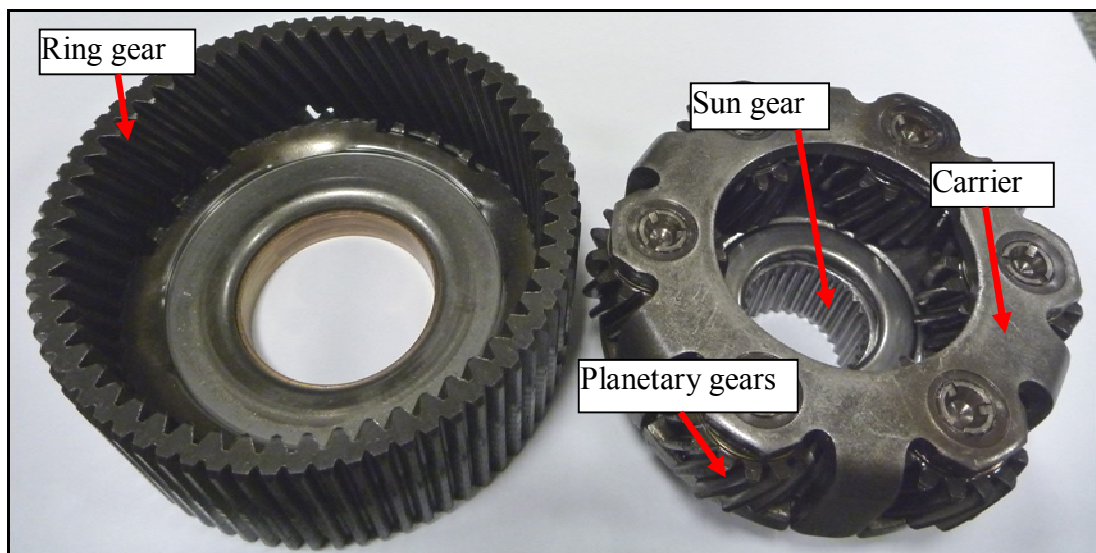


Figure 3.11-1: Planetary gear set from a Ford Transit automatic transmission that could be used in future wheel hub motors.

With a redesign of the front uprights to apply the brake rotors to the inside of the wheels as all preceding UWA Motorsport vehicles operate, the concept could be applied easily to the front wheels as well. This would allow for the use of smaller motors on each wheel and reduce the unsprung mass per wheel while still delivering the same overall vehicle power. Each wheel can have independent acceleration and regenerative braking which will allow for even further development of advanced traction control and driver assistance.

### 3.12 Postponement of Wheel Hub Concept

The wheel hub motor design was conceived using high power density motors that were designed for large model aircraft. As the REV FSAE team intended to use the motors for an automotive application there were several issues that needed to be overcome.

The absence of start-up torque took the electrical team to last month of the project to resolve using Hall Effect sensors on the HXT motors. Only at this stage could the larger Plettenberg motor be ordered as it was confirmed that the required start-up torque was achievable using Hall Effect sensors with this inverted style of electric motor. However by this late stage the suppliers required four weeks to manufacture these motors and a further two weeks to deliver the item to Australia from Germany. Other suppliers of similar motors were sought, but the same month-long lead time was encountered due to the low volume of the product for the model aircraft industry. Alternative motors were researched but nothing could be found that met the power and torque requirements in the compact wheel hub motor arrangement, yet the deadline to produce a drivable vehicle was weeks away.

Given that the low cost designs produced could not adequately protect the motor against overheating and the high levels of vibration expected as unsprung mass, this was perhaps the best outcome because there was a high chance that the motors, valued at \$2000 each with controller, would be destroyed during testing. The deadline to produce a driveable vehicle by the end of the semester still existed so the inboard design initially suggested as an alternative to the wheel hub motor drive at the project's inception became the focus in the last weeks of the project.



#### 4. Inboard Drive Design

This section describes the requirements, design and evaluation of the inboard drive system developed for the REV FSAE vehicle, still bound by the requirements of section 3.3.

The inboard design was not limited by the same physical constraints so larger motors could be used. A new investigation was carried out with the renewed set of constraints to determine the most suitable motors to drive the vehicle. The Rudimentary Design Process was again employed and the possible arrangements investigated.

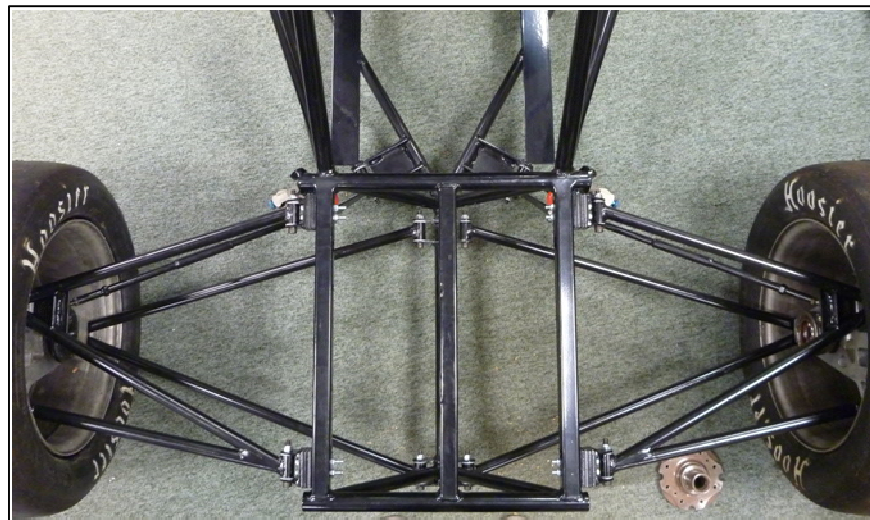


Figure 4-1: Abundance of space for the inboard drive mechanism.

The most simplistic solution was to retain the differential from the 2001 petrol setup on the vehicle and use a large electric motor in the place of the original petrol motor. However the REV FSAE team intended to use one motor per rear wheel to utilise a steering and traction control system which had been in development for the wheel hub concept. This system would sense the steering wheel angle; the velocity of each wheel and acceleration of the vehicle to adjust the current delivered to each motor for optimal traction.

The motor chosen was the Mars ME0201013001: a sensed, brushless DC pancake style motor (figure 4-2) that supported regenerative braking. The motor has the following specifications (Mars 2007):

Weight: 11kg  
RPM Range: 0-5000RPM  
Nominal Voltage: 48VDC  
Continuous Power: 5kW approx  
Peak Power: 10kW approx

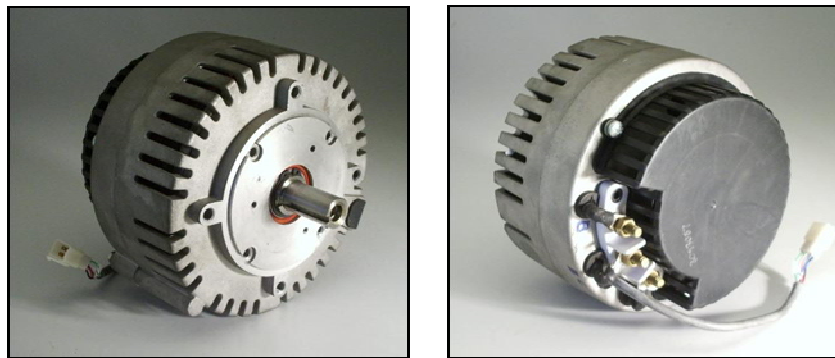


Figure 4-2: Pancake style Mars ME0201013001 used for the inboard design (Mars 2007).

Both single and two stage design were investigated in adjacent and inline motor arrangements.

#### 4.1 Adjacent Two Stage

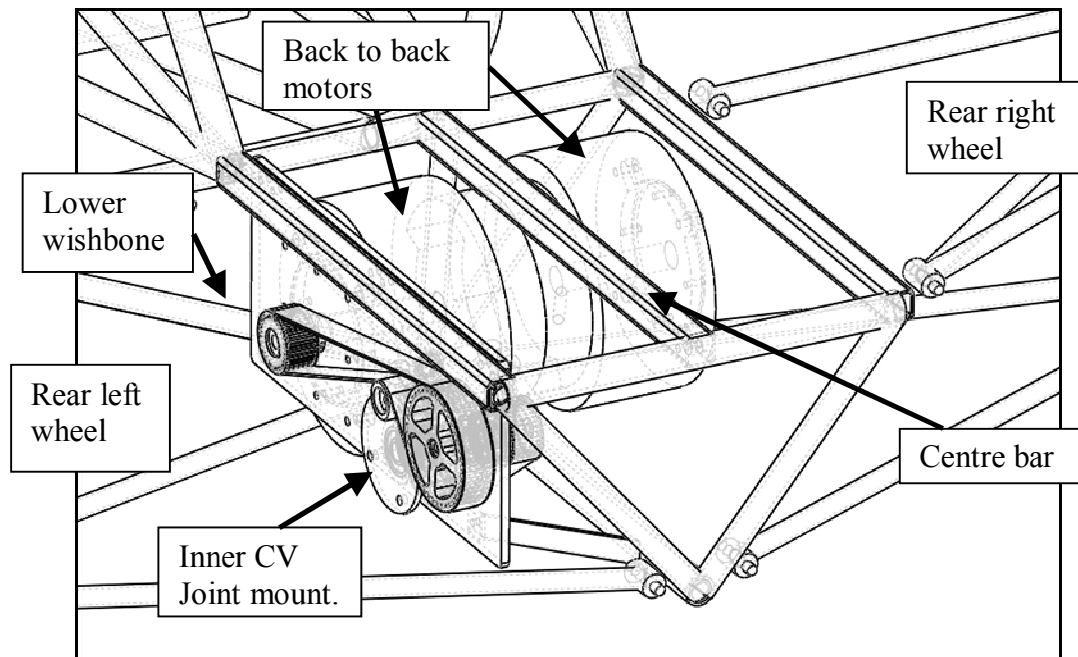


Figure 4.1-1: two motors run back to back – right motor assembly not shown.

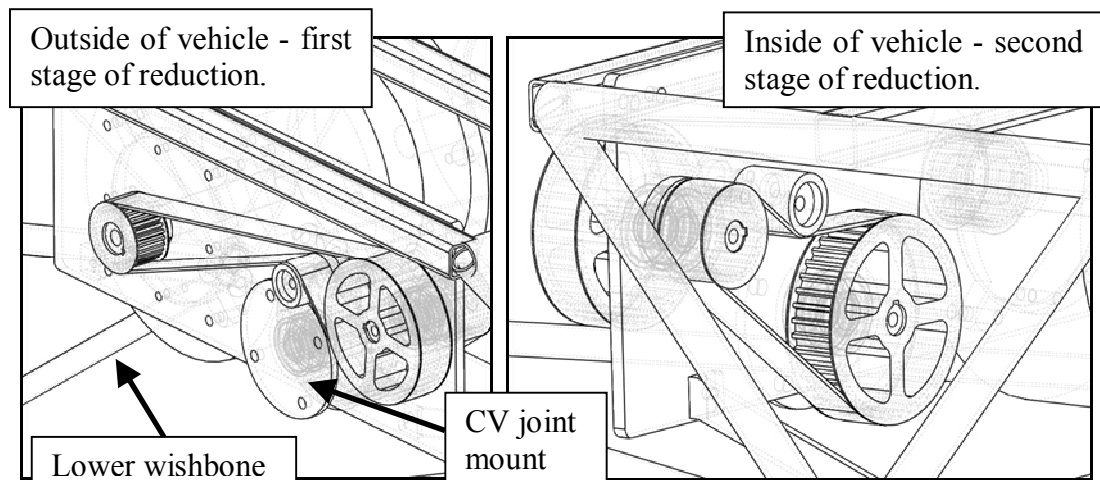


Figure 4.1-2: closer view of the reduction.

The two stage arrangement shown in figures 4.1-1 and 4.1-2 allows the motors to sit as close as possible to the centre of the vehicle. Modelled in Solidworks was the quickest way to modify the arrangement and accurately test for clashes. It was found to have the following disadvantages:

- Required the motors to sit low so that they do not clash with the rear centre bar, which in turn limits the motion of the lower wishbone.

- Could potentially affect cooling as the motors must run back to back with only 5mm separation.
- Long belt required in the first stage pulley reduction to avoid the CV joint mount.

#### 4.2 Inline Phase 1

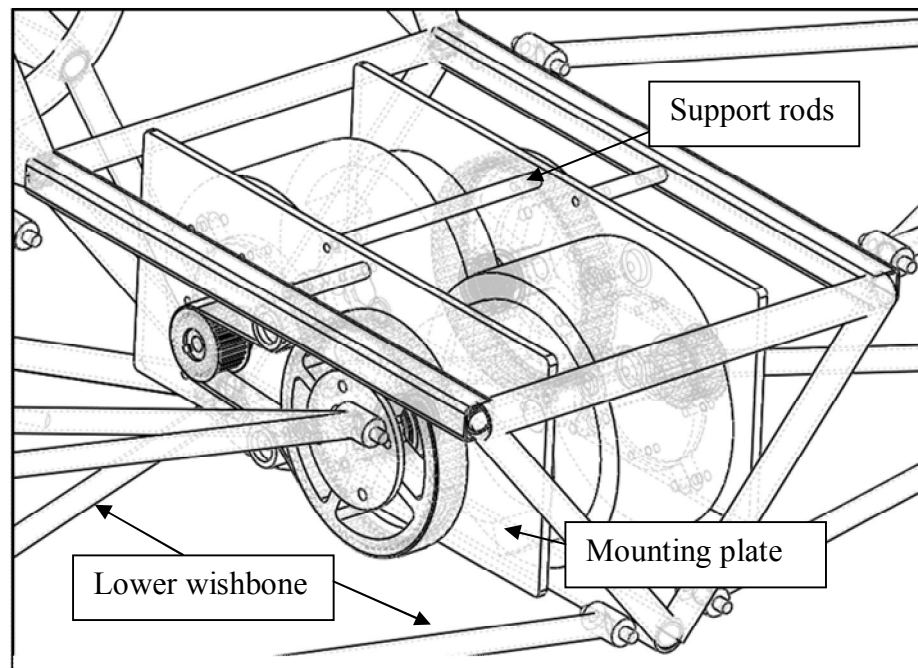


Figure 4.2-1: Single stage inline reduction.

The same two stage design was attempted with the motor inline rather than adjacent to increase the motor-wishbone clearance. The single stage inline design was found to be a better solution as it used the least components and allowed for the greatest wishbone travel. It also allowed for more airflow between the motors, and offered more support points for the mounting the plate to the chassis.

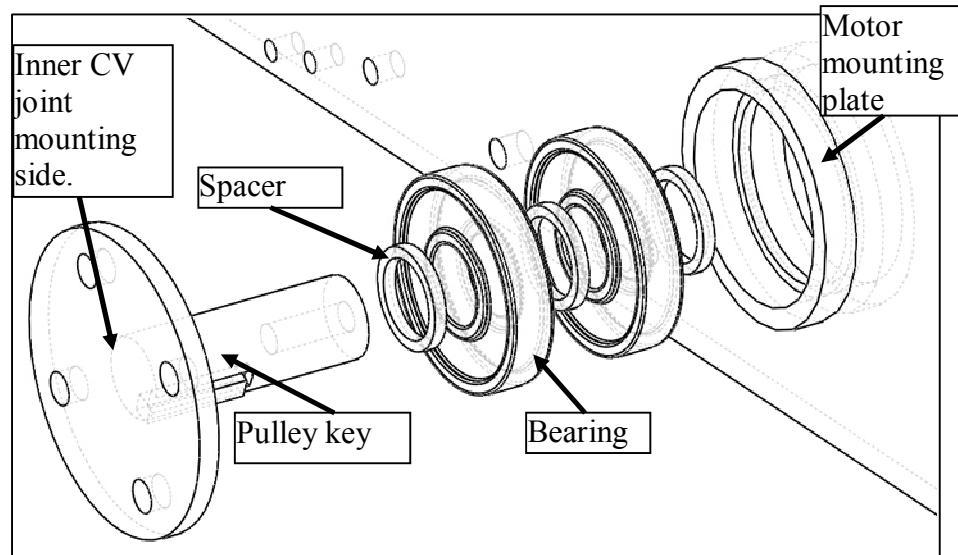


Figure 4.2-2: Initial inboard main pulley mounting.

The driven pulley would be supported by two bearings separated by spacers and pressed into a tubular housing with a central shoulder as shown in figure 4.2-2. The pulley would hold one side in while the other side would be bolted to press the assembly together and locate the bearings.

It required further reinforcing with support bars to prevent lateral movement, and shielding for safety and to prevent debris entering the pulleys and motors. Additionally it required idlers around the driving pulley for the power and torque demand.

#### 4.3 Inline Phase 1 Stress Analysis

A stress analysis was performed on the plate and the rear structure of the vehicle to assess the strength of the assembly with the weight of the motors and belt tension and bending moment.

The following assumptions were used in the stress analysis:

- The axial plunging movement of the CV joint is negligible compared to the other loads so has been omitted from the analysis.
- The bolt tension between components is sufficiently high such that the contact region can be approximated as a bonded contact.

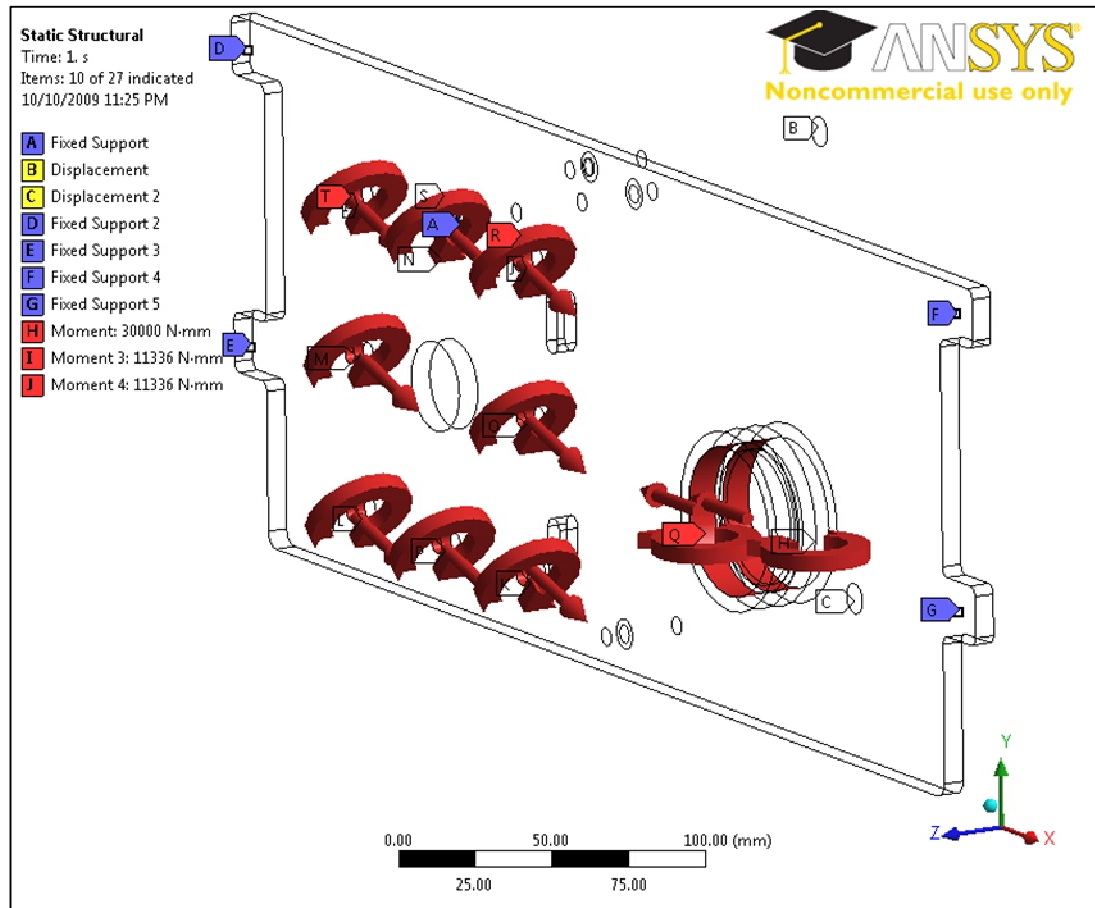


Figure 4.3-1: Resultant forces and moments used in the stress analysis.

The stress model was modified to a single plate by applying a displacement restriction at point B in the Z-axis to simulate equal and opposite rest of the connected structure. This reduces the user input as each load and support does not need to be repeated, as well as reducing the processing time as only half of the model is meshed and analysed.

The applied forces are shown in figure 4.3-1. The combined effects of the mass of the motors and the belt tension have been applied as force vector and a moment vector. The maximum recommended belt tension of 1500N has been used as the applied force to both the motor mounting bolts and the driven pulley. These forces are applied at a distance from the face of the plate, so the resulting moment has also been applied and distributed as shown in figure 4.3-1. A conservative value of 300N has been distributed across the plate bolts to account for mass and wheel hop, as well as a downward moment of 75Nm because the motor centre of mass acts at a distance of 70mm from the plate. The same process has been applied to the driven pulley with an applied force of 1500N and resulting moment of 30Nm because belt tension acts at a distance from the face of the plate.

Due to the limitations of the ANSYS program, the loading assumes the whole cylindrical surface of the bolt hole carries the load. However in the actual physical case, only the side in which the force is directed feels the applied pressure.

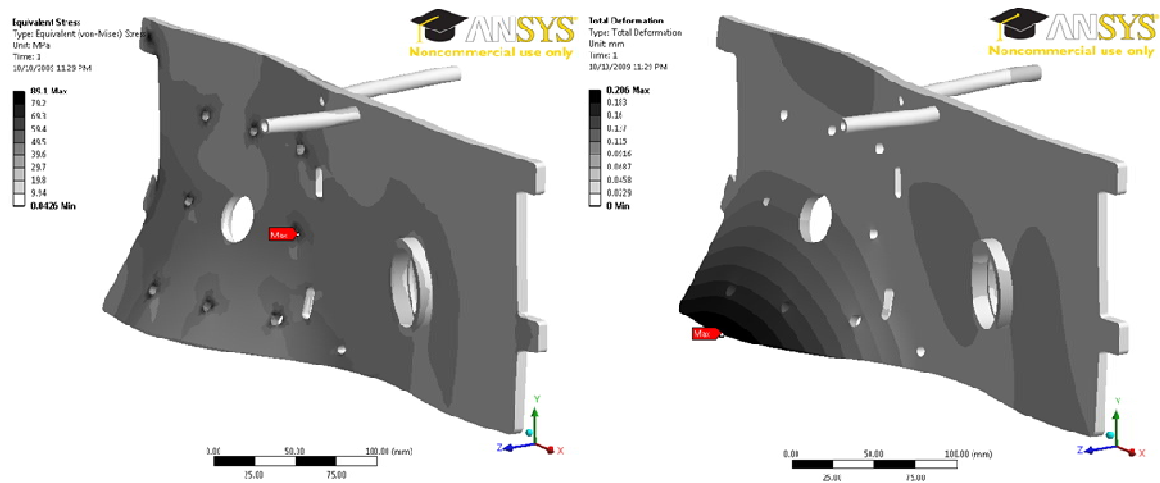


Figure 4.3-2: Von-Mises equivalent stress (left) and maximum displacement (right).

The resulting von-Mises equivalent stress and total displacement plots in figure 4.3-2 show that even with highly conservative values, the maximum stress is 90MPa which is below the 276MPa yield strength of the 6061 aluminium alloy. The maximum displacement is only 0.2mm which is within the allowable pulley misalignment so performance should not be affected (Gates 2007d).

The same unrealistically high stress concentrations were found when modelling bolt holes as fixed supports in ANSYS, so as for the battery cage the bolt holes have been modelled as fixed points in space. It can be seen that this leads to unrealistic twisting deformation of the tabs in directions that would be physically constrained.

The omission of the motor from the stress analysis has resulted in an unexpected deformation in the flexible corner of the plate. This is due to the conservative high motor moment that is applied. In the real physical situation, the motor would restrain all eight holes from displacing in this manner. This would reduce the maximum deflection; the potential for belt misalignment, and also reduce the maximum stress at the bolt hole as this is where the plate begins to bend.

#### 4.3.1 Refinement of Inline Phase 1

Based on the results of the stress analysis and further discussion with workshop technicians regarding the practicality of the design, the following improvements were made:

- The main pulley was brought further to the centre of the plate to reduce the angle on the CV joints.
- The two idlers were replaced with a single adjustable tensioner.

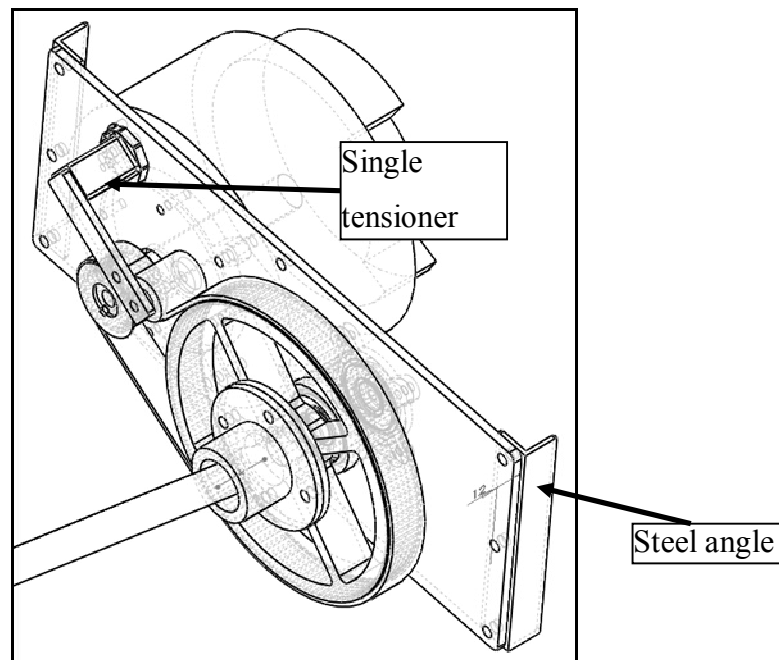


Figure 4.3.1-1: single side of the updated inline pulley design.

- A single larger bearing supported by webbing and captured by a cover plate was used rather than two bearings separated by spacers and a shoulder.
- Angle steel was used at the edges to give the mounting plate increased rigidity instead of tabs.



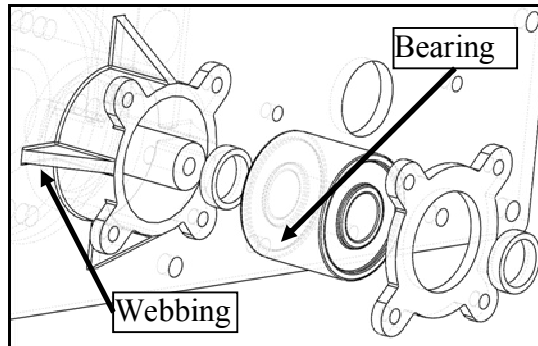


Figure 4.3.1-2: Updated pulley bearing mounting.

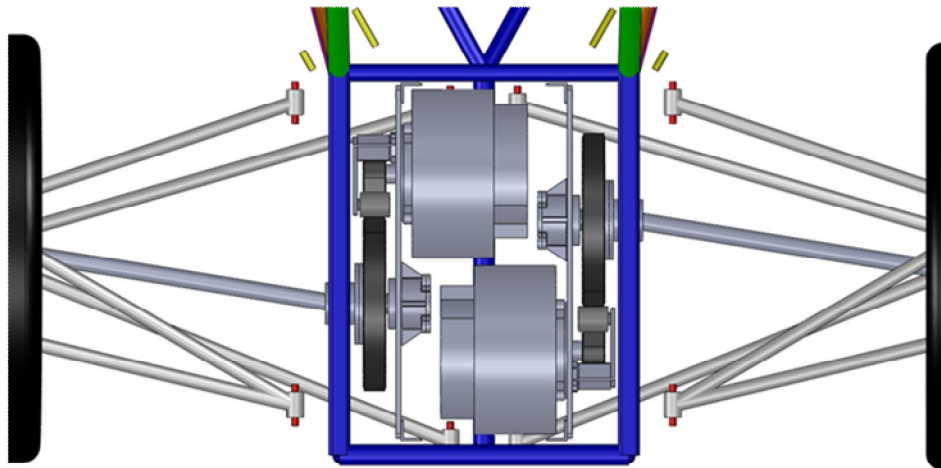


Figure 4.3.1-3: Top view of the inline pulley design.

Only the exposed design is shown for clarity. For safety there is an aluminium shield that covers the top, side and bottom of the motors from debris, and also for driver safety in case of failure.

#### 4.4 Inline Phase 2

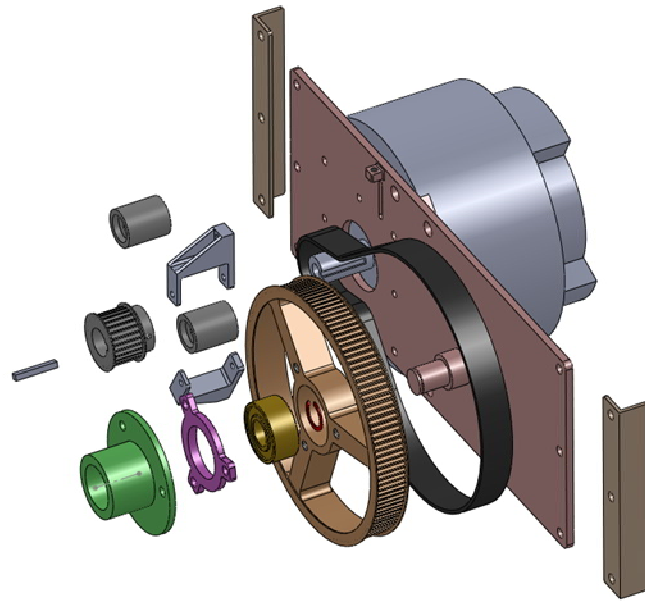


Figure 4.4-1: Exploded view of the final assembly.

A second review of the practicality of design phase 1 was conducted, and a more compact solution found that reduced the part count and the bending moment on the large pulley bearing. Rather than creating a separate housing for the bearing and using a shaft that the CV joint and large pulley mount to over a keyway, the bearing would be pressed into the pulley and run over a shaft that extrudes from the plate as shown in figure 4.4-2. This addresses the greatest disadvantage of design 1: the large bending moment applied to the pulley bearing generated by the belt tension. This was an issue as bearings are design to withstand large axial and radial loads, but none were found that would withstand the bending moment.

The disadvantage of this system is that it requires a pulley machined specifically for this application as there were no stock components found that could be easily modified to suit the intended arrangement. However given that this is a more compact design that uses fewer parts and addresses the critical bending moment that would have most likely lead to the failure of the unit, it is a worthwhile compromise.

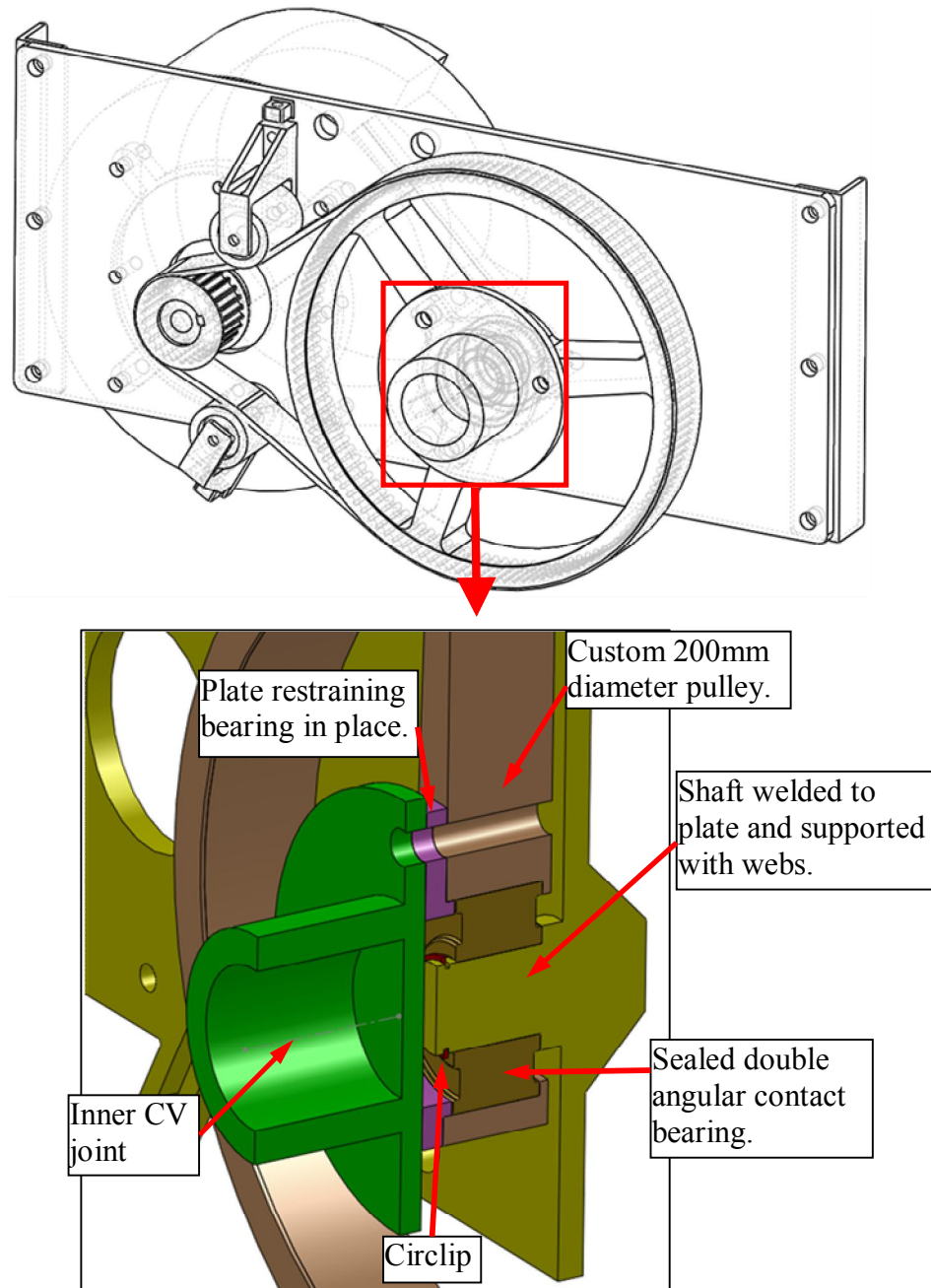


Figure 4.4-2: section view of the plate design addressing the issues of inboard design 1.

This design also uses webs to support the bending moment due to belt tension, but applied to the shaft instead of the bearing housing as shown in figure 4.4-2. This reduces the protrusion from the back of the plate and allows the motors to sit closer together, reducing the space the total arrangement occupies. Ridges were also applied across the back of the plate to increase stiffness as shown in figure 4.4-3.

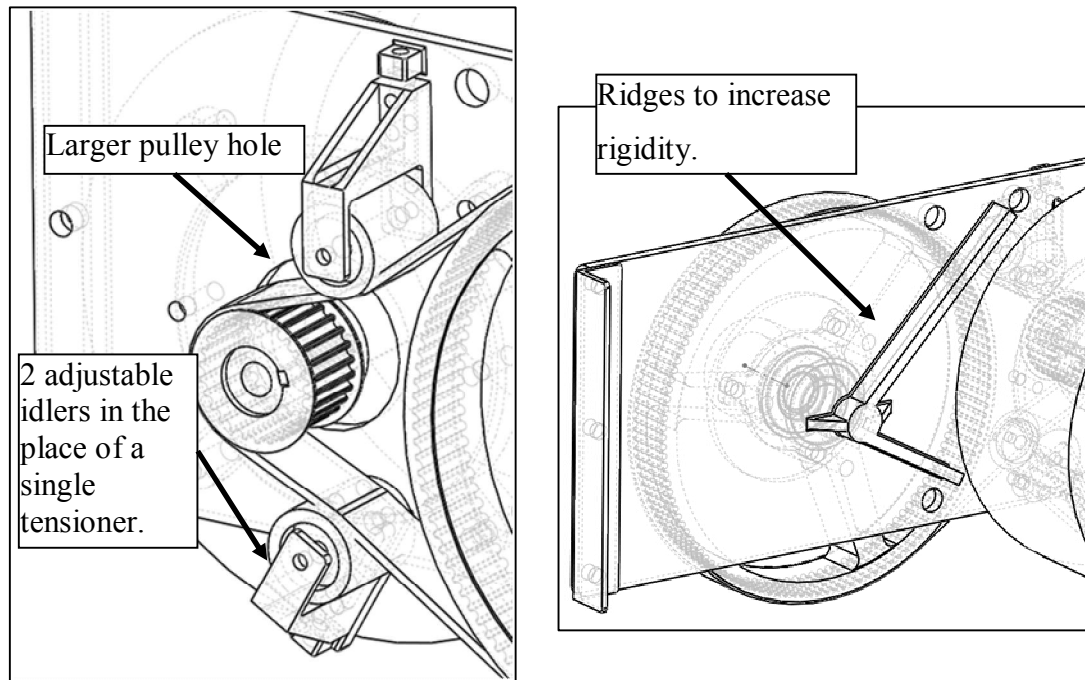


Figure 4.4-3: adjustable idlers, larger driving pulley hole and ridges to improve design.

The driving pulley hole was increased so that the motor could be detached from the plate without having to remove the driving pulley. Figure 4.4-3 shows that the stock tensioner was removed because it was too flexible to hold its position on the belt and deliver the required belt wrap. In its place, two adjustable idlers were designed which would serve to adjust for variable belt lengths as well as give the required belt wrap around the smaller driving pulley. A larger and exploded view of the assembly is shown in appendix E.

#### 4.5 Inline Phase 2 Stress Analysis

A conservative dynamic loading factor of 3 has again been used on the weight of the motor. The loads and bending moments due to the electric motor weight and the belt tension has been distributed across the 8 mounting bolt holes and the same set of assumptions used as in section 4.3.

Again as per section 4.3, only a simplified half model has been used employing symmetry with a fixed displacement to reflect the equal and opposite connection to the rest of the drive assembly. 6061 aluminium alloy has been used as the material with properties as per the material data sheet provided by supplier Robert Cameron (Alcoa

2006). A convergence test was performed varying the element size and relevance centre until the stress results converged within 5%.

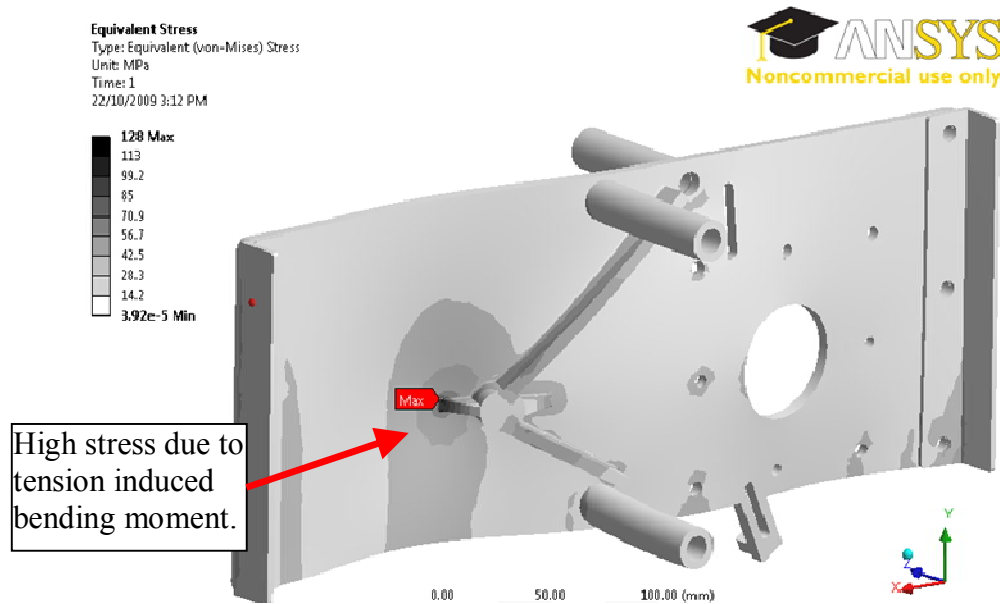


Figure 4.5-1: Inboard view of the maximum von-Mises equivalent stress contour plot.

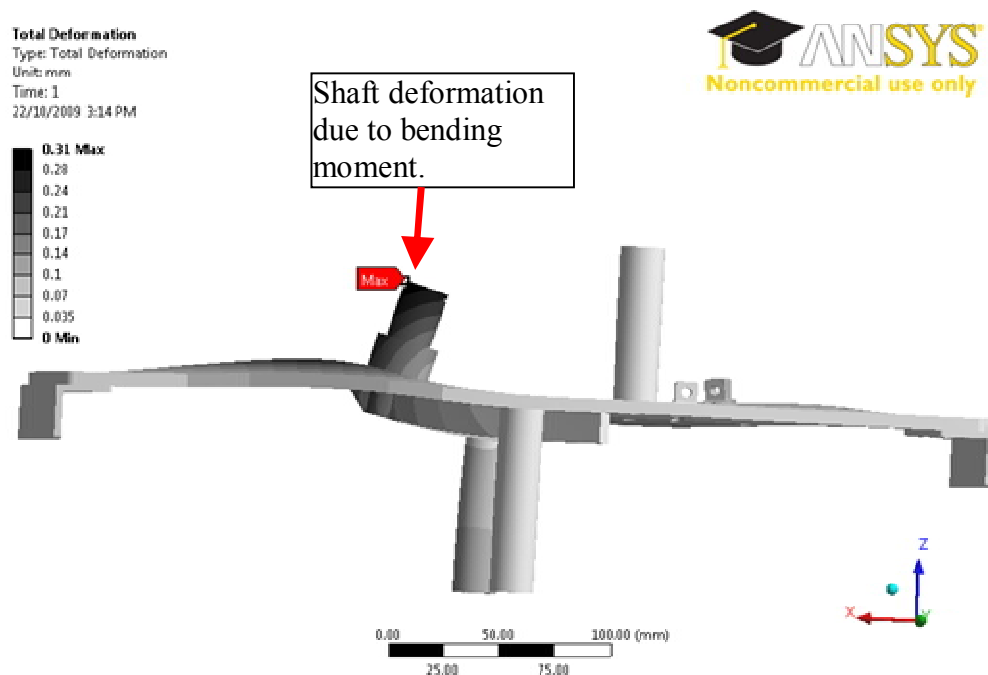


Figure 4.5-2: Top view of maximum deformation contour plot.

With three times dynamic amplification of motor weight and resulting moment, as well as 1500N of belt tension, the highest equivalent von-Mises equivalent stress was found to be 128MPa, less than half of the 276MPa yield strength of the 6061 alloy with a

maximum deflection of 0.31mm. This may suggest that the 6mm plate that is being used is excessive, however the thickness is a safety margin for the spontaneous changes made without stress analysis that are likely during the construction phase. Also given that this is the first electric iteration of the vehicle, the added material leaves scope for future modifications.

#### 4.6 Bearing Selection

The bearing chosen for the driven pulley needed to be able to withstand radial loads of up to 1500N due to the belt tension, as well as the axial plunging loads of the connected CV joints. Additionally it needs to be sealed because the arrangement in figure 4.4-2 is exposed to the elements.

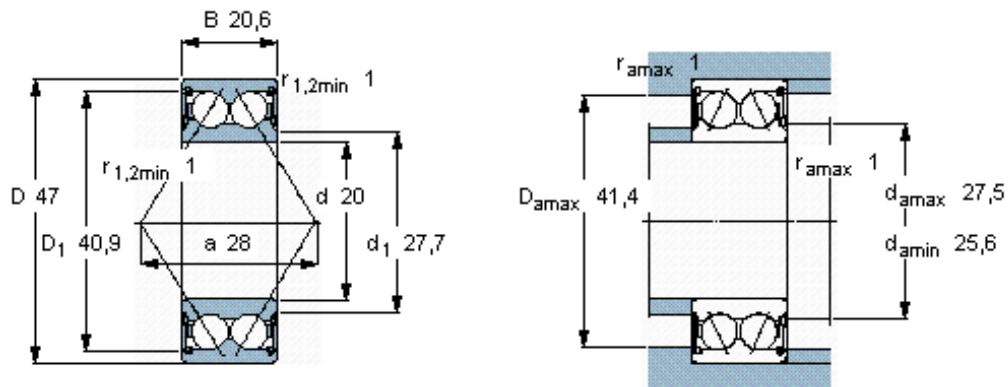


Figure 4.6-1: SKF 3204 A-2RS1TN9/MT33 sealed double angular contact bearing chosen for the driven pulley bearing (SKF 2009).

For this application, the SKF sealed double row angular contact bearing has been chosen shown in figure 4.6-1. It will withstand up to 34Nm of applied moment which is expected if there is significant deflection of the shaft. The outside is pressed into the pulley and allowed to run over the shaft. It is restrained on one side by a shoulder on the shaft and on the pulley, and on the other side by a plate and circlip as shown in figure 4.4-2.

#### 4.7 Pulley & Belt Selection

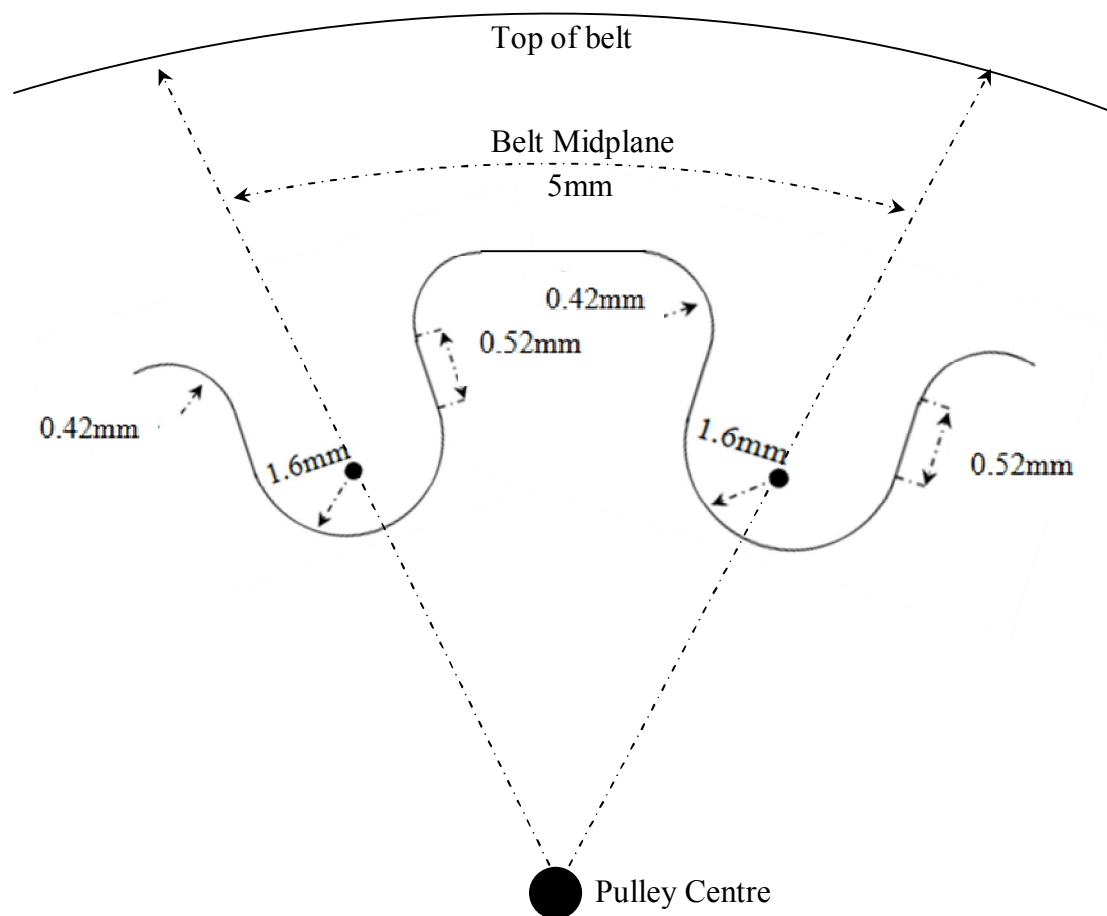


Figure 4.7-1: 5mm pitch synchronous pulley dimensions used in pulley design (not to scale).

The pulley chosen is the 25mm wide, high torque curvilinear HTD style with the standard dimensions shown in figure 4.7-1. A 5mm pitch is the minimum required for the smaller 40mm diameter pulley, however is not readily available for the larger 200mm pulley in a suitable light weight material. Synchronous pulleys are available locally, but manufactured from cast iron which is not suitable for an FSAE vehicle because of its high weight.

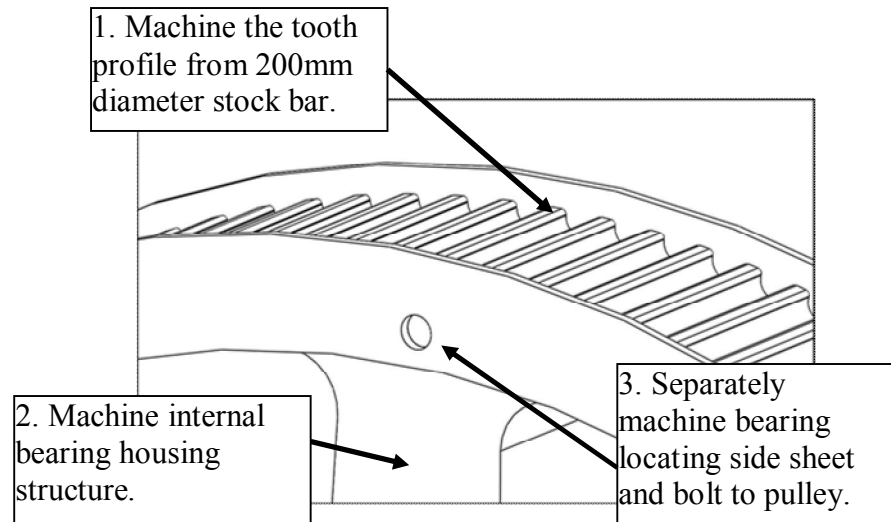


Figure 4.7-2: manufacture of the 5mm pitch synchronous pulley.

Even if a stock 200mm pulley was sourced, the centre would need significant machining and modification to accept the bearing with an interference fit. For this reason it is recommended that a custom pulley be manufactured from bar stock because the HTD profile is highly desirable for the application and can be easily machined. The round profile of the teeth can be machined then plates added to the side to locate the belt as shown in figure 4.7-2.

The belt chosen is a matching industry standard 5mm pitch HTD curvilinear style belt that is low cost and readily available with a maximum recommended tension loading of approximately 1500N (Gates 2009e). Depending on the final arrangement, the belt length is expected to be between 740mm and 760mm, which can be adjusted for using the idlers.



#### 4.8 Drive shafts & CV Joints

An investigation was carried out into the suitability and usability of the drive shaft and CV joint components left over from the 2001 vehicle build, as well as what remains on the vehicle.

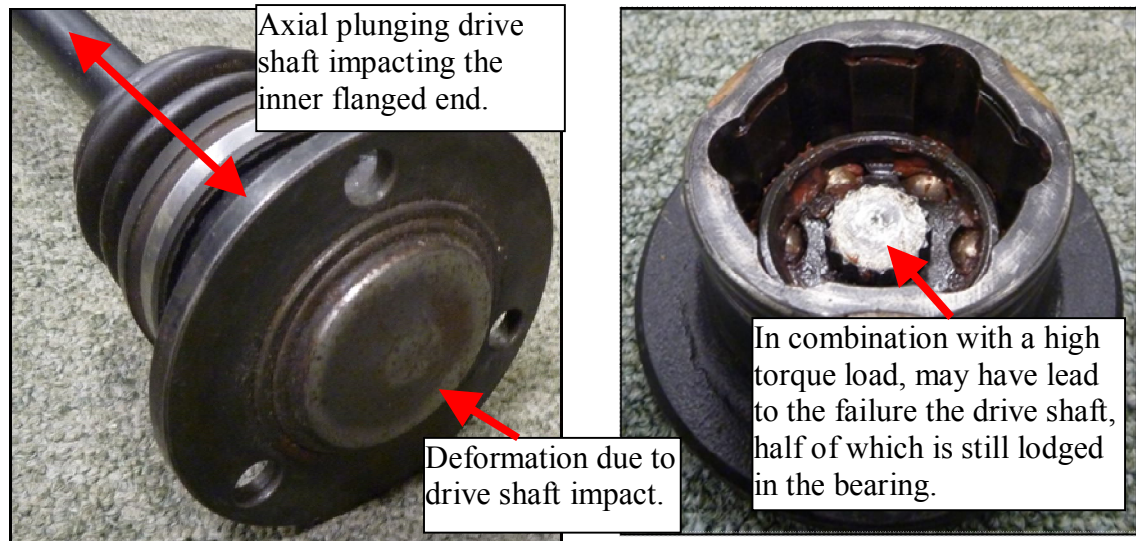


Figure 4.8-1: Failure of the flanged axial plunging inner CV joint.

It is suggested that the new inner and outer CV joints be purchased for the rebuild because the current joints are of the smaller type using the uncommon 17 and 18 spline which will require two new drive shaft splines cut at an approximate cost of \$600. Further to this, the selection of available drive shafts left from the 2001 build are all of the 20mm diameter, 19 spline type which is common to small vehicles and for which there is an abundance of cheap, commercial CV joints available.

Given that it is approximately twice as expensive to cut a spline as it is to buy an entirely new CV joint, it is suggested that the available 19 spline drive shafts be used, and new CV joints purchased at approximately \$70 each. Also as figure 4.8-1 of the current setup shows, the flange deformation due to drive shaft impact on the inner CV joints suggests that there is not enough drive shaft travel using the current small type of CV joint on the vehicle.



Figure 4.8-2: Inner CV joint modification. (KML Bearing 2009)

Figure 4.8-2 shows that the purchased inner CV joint will need to be cut and a flange welded in the place of the splined shaft that would typically connect to inboard of the vehicle. This is so that the CV joint can later be detached and the whole unit removed from the vehicle. Once the inboard motor assembly is manufactured and the CV joints purchased, the final step is to load the suspension with all the mass including driver and determine the length of drive shaft required, expected at approximately 400mm.

#### 4.9 Evaluation

The result is a stress analysed, optimised unit that meets the design requirements defined in section 3.3.

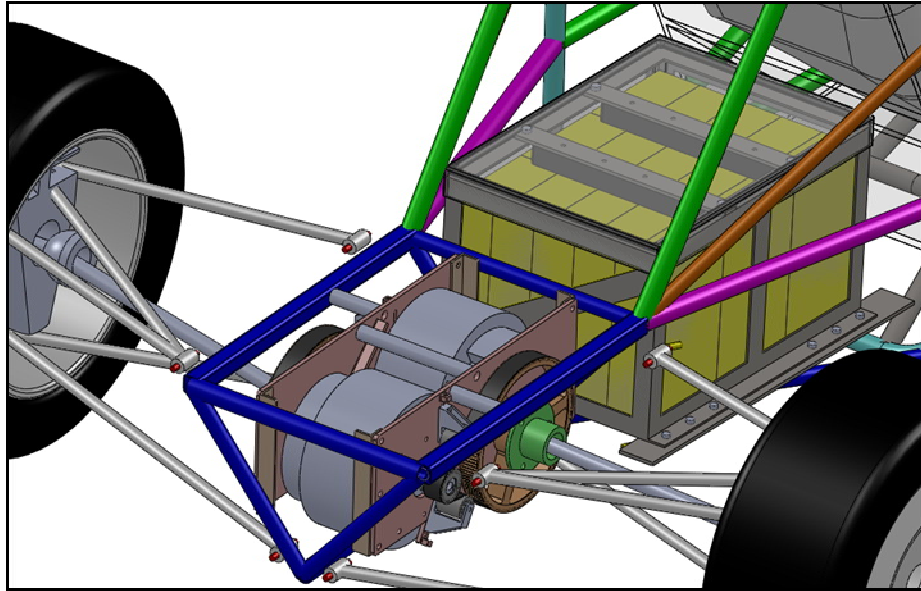


Figure 4.9-1: Final assembly showing drive system and battery cage in their location with the aluminium sheet is omitted for clarity.

- **Low cost** - Using a low cost motor and primarily industry standard belts, bearings and CV joints.
- **Easily manufactured** - simple plate geometry with majority drilled holes. The only CNC machining required is for the driven pulley.
- **Easily serviced** - modular design allows the whole unit to be removed by unbolting CV joints and motor mounting plate from the steel angle.
- **Waterproof** - motors are waterproof and whole unit will be shielded with aluminium sheet to keep out debris.
- **Comparable performance to '01 petrol setup** - similar weight and distribution as batteries take place of petrol motor, and electric motor takes place of differential and rear brake. Regenerative braking can be used in the place of existing friction brakes.

#### 4.10 Future Work

This assembly needs to be manufactured, which will have a whole host of practical complications that will only become evident during construction, in spite of the author's best efforts to foresee and mitigate any potential issues.

When the funds become available, consideration should be given to higher power density motors and light weight CV joints for increased acceleration. The electric motors can be overdriven beyond their rated peak current and power for short bursts of time; however this is partially limited by overheating so an active cooling system through either air or water cooling should be investigated. Additionally, rear friction brakes are still required for the FSAE competitions, so this will need to be investigated prior to competition entry.

#### 4.11 Safety

Elements of safety were described throughout the document, but will be summarised here for clarity. The design has been produced with manufacturing and operation in mind. The majority of components are easily machined with basic equipment, and do not have complex geometry or intricate features. The design has been stress analysed with excessive loading and assembled so that the weakest component in the running assembly will be the belt, which is the least harmful to the driver or a bystander. Even so, the entire unit has been covered in aluminium sheet in the event of such a failure. The entire drive unit is modular and should be removed from the vehicle for testing and analysis.

## 5 UWAM and REV FSAE

The hybrid-electric and full-electric FSAE competitions are unique opportunities for The University of Western Australia to assert itself as a leader as the world undergoes a shift in mindset to electric vehicles. Ideally this should be as a partnership between REV and the UWAM team.

While the REV team has a developed BMS and charging systems for the electrical vehicles it has converted, it is still in its infancy in terms of vehicle design. A competitive entry into the electric FSAE competitions would only be successful through a partnership between UWAM and REV.

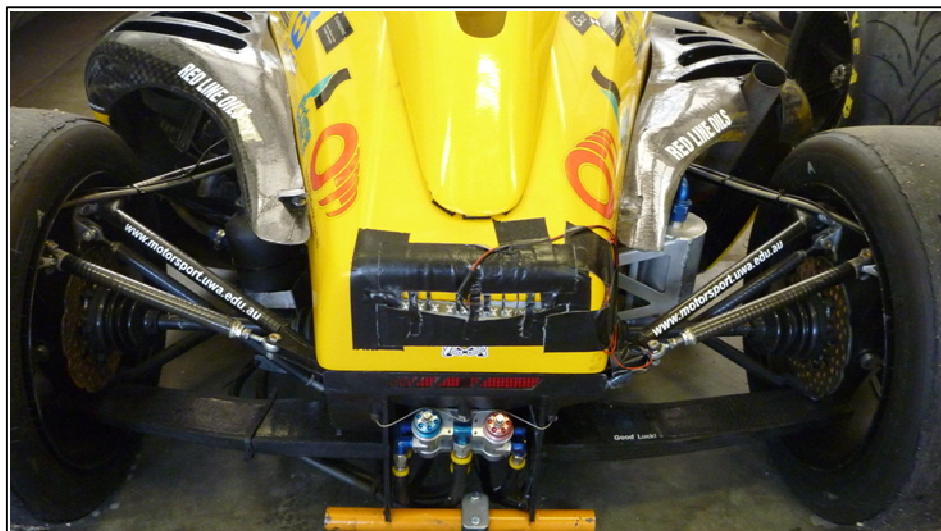


Figure 5-1: Rear assembly of the 08 UWAM FSAE vehicle, the calibre of which REV SAE will need to produce to be competitive.

UWAM possess 9 years of highly successful FSAE vehicle development; financial and administrative systems, and a loyal base of sponsors earned through competitive success. It has relationships with vendors; a dedicated mechanical workshop, trailers with the required tools and testing equipment, none of which REV FSAE possesses. The level of chassis and suspension system required to compete successfully in the current FSAE competition by the UWAM team is the result of 9 years of development, as shown in figured 5-1 and 5-2. It is unrealistic to expect the REV FSAE team to again start from the beginning and independently produce a competitive chassis and suspension system to the calibre that UWAM has taken the past 9 years to refine.



Figure 5-2: Construction of the 09 UWAM FSAE chassis.

The UWAM team members are enthusiastic about extending their mechanical knowledge of performance vehicle design to the emerging electric vehicle competition. The REV FSAE team members are equally eager to partner their electrical system knowledge with UWAM because both teams of students understand how attainable, unique and valuable the resulting vehicle of such collaboration will be.

Ideally two carbon fibre monocoque chassis, suspension and steering systems could be produced for both petrol and electric competitions because the weight distribution can be kept very similar between the two drive systems. Alternatively a single chassis could be produced that is designed to accept both drive systems. The petrol engine and fuel tank could be removed through the rear then electric motors and batteries added in their place. All other major mechanical components including chassis, steering and suspension would remain structurally unchanged or could be easily adjusted. With the potential for such innovation and success, there is little justification for the arbitrary separation and competition between REV and UWAM.

## 6. References

Agni Motors 2009, *95 Series Motor*, Available from:

<[http://www.agnimotors.com/home/index.php?option=com\\_content&task=view&id=5&Itemid=60](http://www.agnimotors.com/home/index.php?option=com_content&task=view&id=5&Itemid=60)>. [6 April 2009]

Alcoa 2006, *Understanding Extruded Aluminium Alloys – 6061*. Alcoa Inc., Available from: <[http://www.alcoa.com/adip/catalog/pdf/Extruded\\_Alloy\\_6061.pdf](http://www.alcoa.com/adip/catalog/pdf/Extruded_Alloy_6061.pdf)>. [27 June 2009]

Boughtwood, M 2008, *Motor with individually controlled stator coils*, European Patent GB2440251 (A)

Callister, WD 2007, *Materials Science and Engineering: An Introduction*, John Wiley & Sons, New York.

Carmody, S 2003, 'Maybe they'll change their name to General Wheel Motors', *Machine Design*, 10 September, p. 30. Available from Academic Search Premier. [2 April 2009].

Cho, S 2006, 'Efficiency of the planetary gear hybrid powertrain', *Journal of Automobile Engineering*, vol 220, pp 1445-1454. Available from: Academic Search Premier. [22 September 2009]

Corke, P 2009, *Vehicle Dynamics of the 2009 REV FSAE Vehicle*, honours thesis, University of Western Australia.

Degarmo, P 2008, *Materials and Processes in Manufacturing*, Wiley, Chichester.

Department of Infrastructure, Transport, Regional Development and Local Government 2006, *National Code of Practice for Light Vehicle Construction and Modification (NCOP)*, Australian Government, Available from: <[http://www.infrastructure.gov.au/roads/vehicle\\_regulation/bulletin/vsb\\_ncop.aspx](http://www.infrastructure.gov.au/roads/vehicle_regulation/bulletin/vsb_ncop.aspx)>. [12 July 2009]

EV Parts 2009, *Advanced DC #140-07-4001*, Available from:

<<http://www.evparts.com/prod-MT2110.htm>>. [7 April 2009]



Formula Hybrid 2009a, *Formula Hybrid Competition Rules and Scoring*, Formula Hybrid, Available from: <<http://www.formula-hybrid.org/pdf/Formula-Hybrid-2010-Rules.pdf>>. [10 March 2009]

Formula Hybrid 2009b, *Formula Hybrid Electrical Safety Rule Notes*, Available from: <<http://www.formula-hybrid.org/pdf/electrical-notes-rev1.pdf>>. [10 March 2009]

Gates 2009a, *Belt Drive Preventative Maintenance and Safety Manual*, Gates Corporation, Available from: <[http://www.gates.com/catalogs/file\\_display.cfm?file=PT\\_beltPMweb.PDF&thisPath=gates\catalogs](http://www.gates.com/catalogs/file_display.cfm?file=PT_beltPMweb.PDF&thisPath=gates\catalogs)>. [24 August 2009]

Gates 2009b, *Differences in Synchronous Belts*, Gates Corporation, Available from: <<http://www.gates.com/facts/documents/Gf000282.pdf>>. [2 September 2009]

Gates 2009c, *Industrial Belts Catalogue*, Gates Corporation, Available from: <[http://www.gates.com/catalogs/file\\_display.cfm?file=SynchronousBelts.pdf&thisPath=gates\catalogs](http://www.gates.com/catalogs/file_display.cfm?file=SynchronousBelts.pdf&thisPath=gates\catalogs)>. [14 July 2009]

Gates 2009d, *Synchronous Belt Failure Guide*, Gates Corporation, Available from: <[http://www.gatesprograms.com/assets/ptsavings/Belt\\_Failure\\_Analysis.pdf](http://www.gatesprograms.com/assets/ptsavings/Belt_Failure_Analysis.pdf)>. [5 September 2009]

Gates 2009e, *Synchro-Power - Linear Positioning & Motion Control*, Gates Corporation, Available from: <[http://www.gates.com/catalogs/file\\_display.cfm?file=gatesmectrolcatalog\\_3\\_07.pdf&thisPath=gates\catalogs](http://www.gates.com/catalogs/file_display.cfm?file=gatesmectrolcatalog_3_07.pdf&thisPath=gates\catalogs)>. [20 August 2009]

Gates 2009f, *Tensioning Synchronous Belts*, Gates Corporation, Available from: <<http://www.gates.com/facts/documents/Gf000278.pdf>>. [4 September 2009]

Hobby King 2009, *Turnigy HXT 80*, Available from: <[http://www.hobbycity.com/hobbycity/store/uh\\_viewItem.asp?idProduct=5142](http://www.hobbycity.com/hobbycity/store/uh_viewItem.asp?idProduct=5142)>. [8 April 2009]

Ip, C S 2008, *Battery Restraint System and Performance Evaluation for Renewable Energy Vehicle Project*, honours thesis, University of Western Australia.



KML Bearing 2009, *Inner CV Joint Automotive Bearing*, KML Bearing & Equipment Ltd, Available from: <[http://www.kml-bearing.com/products/bearings/automotive\\_bearing\\_catalogue.jsp?cat\\_id0=141102&pageNo=2](http://www.kml-bearing.com/products/bearings/automotive_bearing_catalogue.jsp?cat_id0=141102&pageNo=2)>. [1 October 2009]

Lightning 2009, *Lightning GT Technical Specifications*, Lightning Car Company, Available from: <<http://www.lightningcarcompany.co.uk/files/Lightning-Spec-Card.pdf>>. [13 June 2009]

Mars 2007, *PMSM Motor ME0201013001 2007*, Available from: <<http://marselectricllc.com/burnishermotor.html>>. [5 April 2009]

Michelin, 2008, *Michelin Reinvents the Wheel*. Available from: [http://www.michelin.co.uk/michelinuk/AfficheServlet?Rubrique=20061224112323&Langue=EN&news\\_Id=23759](http://www.michelin.co.uk/michelinuk/AfficheServlet?Rubrique=20061224112323&Langue=EN&news_Id=23759) [15 April 2009]

Morrigan, A 2009, *Analysis of the 2009 REV Racer Car Suspension*, honours thesis, University of Western Australia.

Nagayo, G 2003, 'Development of an in-wheel drive with advanced dynamic-damper mechanism.' *JSAE Review*, vol. 24 Issue 4, p 477. Available from: Academic Search Premier. [18 April 2009]

Perm Motor 2009, *Perm PMS100*, Available from: <[http://www.perm-motor.de/site/en/products/syn\\_motors.php?linkid=p&linkid2=1](http://www.perm-motor.de/site/en/products/syn_motors.php?linkid=p&linkid2=1)>. [7 April 2009]

Plettenberg 2005, *Plettenberg Predator 37*, Available from: <<http://www.plettenberg-motoren.com/UK/Motoren/aussen/Predator/Motor.htm>>. [8 April 2009]

Siemens, 2006, *Siemens VDO's By-wire Technology turns the eCorner*. Available from: <[http://usa.vdo.com/press/releases/chassis-and-carbody/2006/SV\\_20061016\\_i.htm](http://usa.vdo.com/press/releases/chassis-and-carbody/2006/SV_20061016_i.htm)> [16 March 2009]

SKF 2009, *Product Data - Angular Contact Ball Bearings, Double Row, Seal On Both Sides*, SKF Group, Available from: <<http://www.skf.com/skf/productcatalogue/Forwarder?action=PPP&lang=en&imperial=false&windowName=null&perfid=125003&prodid=125003204>>. [14 October 2009]

Thunder Sky 2009, *Thunder Sky LiFeYPO<sub>4</sub> Power Battery Specifications*, Thunder Sky Energy Group Limited, Available from: <<http://www.thunder-sky.com/pdf/200931791117.pdf>>. [10 July 2009]

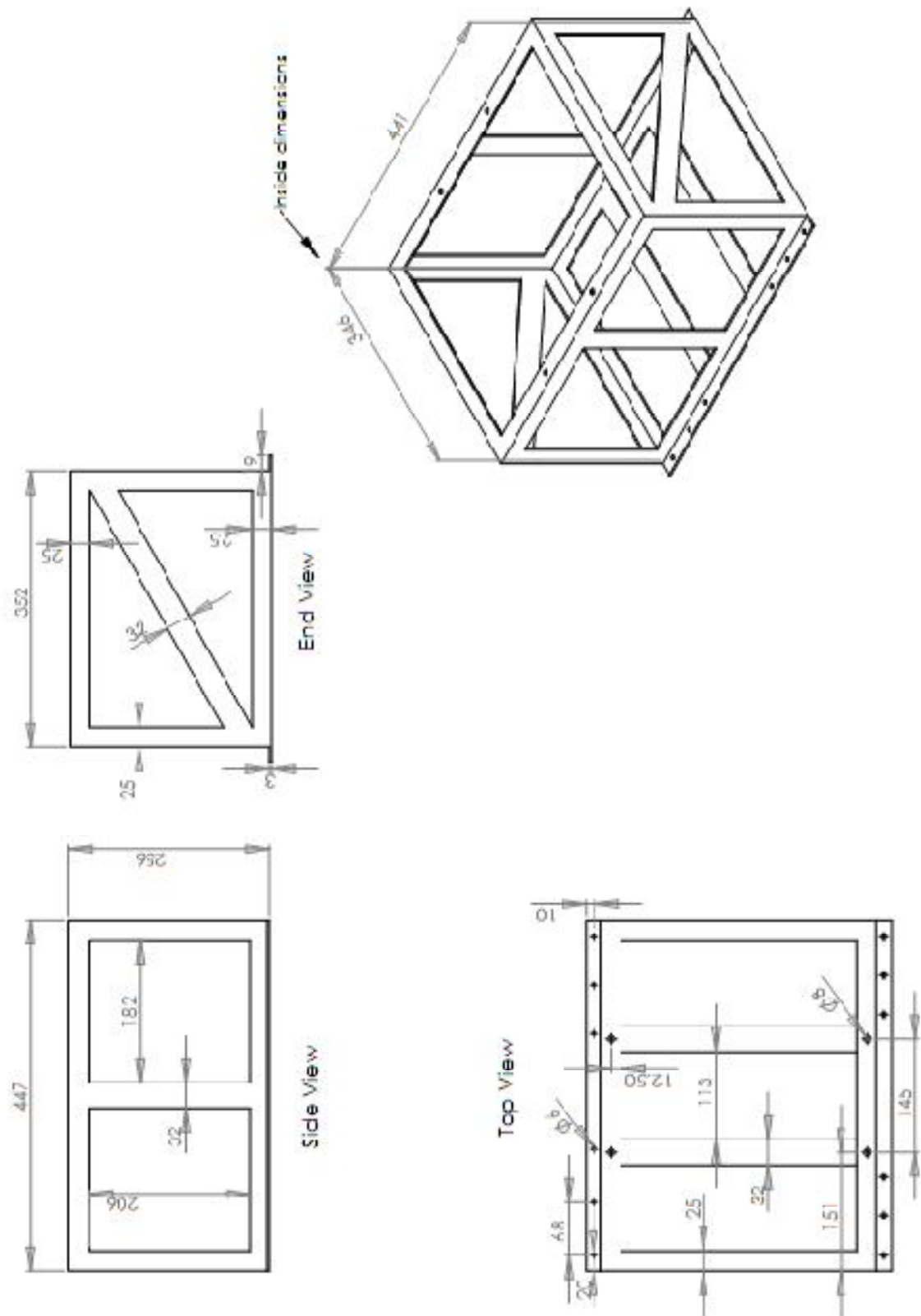
Tietzel, C 2009, *Battery Cage Mechanics for the Renewable Energy Vehicle Project*, honours thesis, University of Western Australia.

Waldron, G 2004, *Kinematics, dynamics, and design of machinery*, John Wiley, Hoboken NJ.

Wright, D 2000, *Design and Analysis of Machine Elements*, lecture notes distributed in Mechanical Design at The University of Western Australia, Crawley in March 2008.

## Appendix

### A: Battery Cage



## B: Structural Steel Strength Certification

OFFICE : 臺中縣后里鄉甲后路702號  
 702, CHIA HOU ROAD, HOU LI SHUNG,  
 TAICHUNG HSIEN, TAIWAN, ROC  
 TEL : (04)25565101 FAX : (04)25566955

**豐興鋼鐵股份有限公司**  
**FENG HSIN IRON & STEEL CO., LTD.**

MILL TEST CERTIFICATE

CUSTOMER NAME: CP MARKETING INTERNATIONAL PTY LTD.  
 SPEC: AS3578.01 G300 MODIFY

CERTIFICATE NO. 1078161-A1-1  
 CERTIFICATE DATE OCT. 06 2008

GOODS DESCRIPTION			TENSILE TEST		CHEMICAL ANALYSIS (%)												
SIZE (mm)	LEN. (m)	QTY	WEIGHT (kg)	HEAT NO.	YP N/mm <sup>2</sup>	TS N/mm <sup>2</sup>	EL (%)	C	Si	Mn	P	S	Ni	Cr	Mo	Al	B
					MIN	MIN	MIN	MAX	MAX	MAX	MAX	MAX	MAX	MAX	MAX	MAX	MAX
MILD STEEL MERCHANT BARS-EQUAL ANGLE BARS																	
B * t																	
65 # 6	9	11	22.929	303397	320.0	440.0	22.0	25	50	160	40	40					
SUB TOTAL		11	22.929		333.0	516.0	23.5	MAX	MAX	MAX	MAX	MAX					
MILD STEEL MERCHANT BARS-FLAT BARS																	
B * t																	
25 # 3	6	3	5.337	303528	320.0	440.0	22.0	25	50	160	40	40					
25 # 3	6	3	4.226	303529	332.0	522.0	25.0	18	18	82	15	20					
25 # 6	6	6	9.516	303529	424.0	558.0	36.0	19	21	86	17	27					
32 # 3	6	8	11.914	303529	424.0	558.0	36.0	19	21	86	17	27					
32 # 6	6	6	9.860	303529	424.0	558.0	36.0	19	21	86	17	27					
SUB TOTAL	6	26	40.863														
Grand Total:	37	BUNDLES	63,792	kg.													

REMARK: The shape and dimensional tolerances of hot rolled steel are according to JIS.

QC-09-04

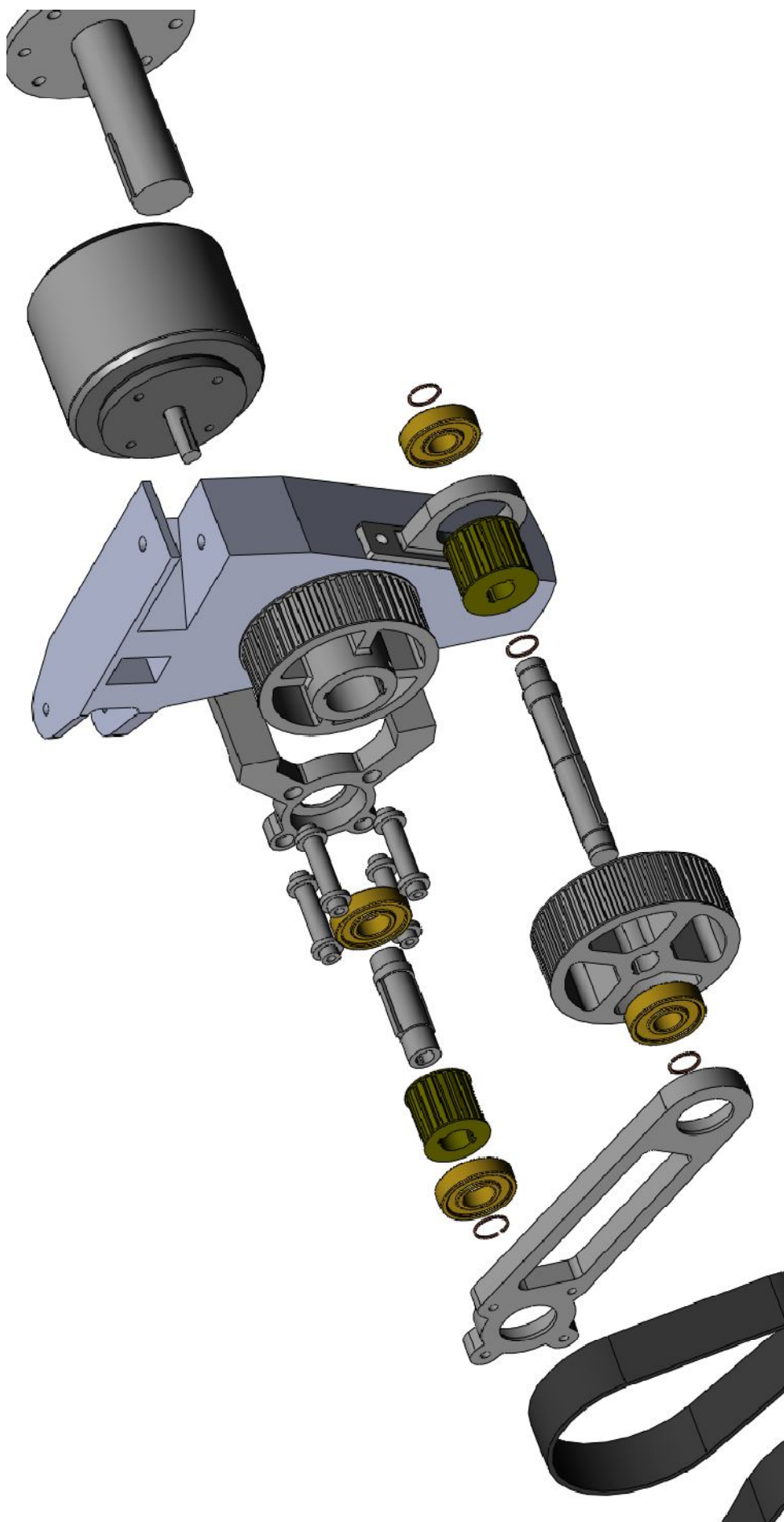
MANAGER  
 METALLURGICAL  
 R&D DEP.

郭志毅

WE HEREBY CERTIFY THAT THE MATERIAL DESCRIBED HEREIN HAS BEEN MANUFACTURED AND TESTED WITH SATISFACTORY RESULTS IN ACCORDANCE WITH THE REQUIREMENT OF THE ABOVE MATERIAL SPECIFICATION.

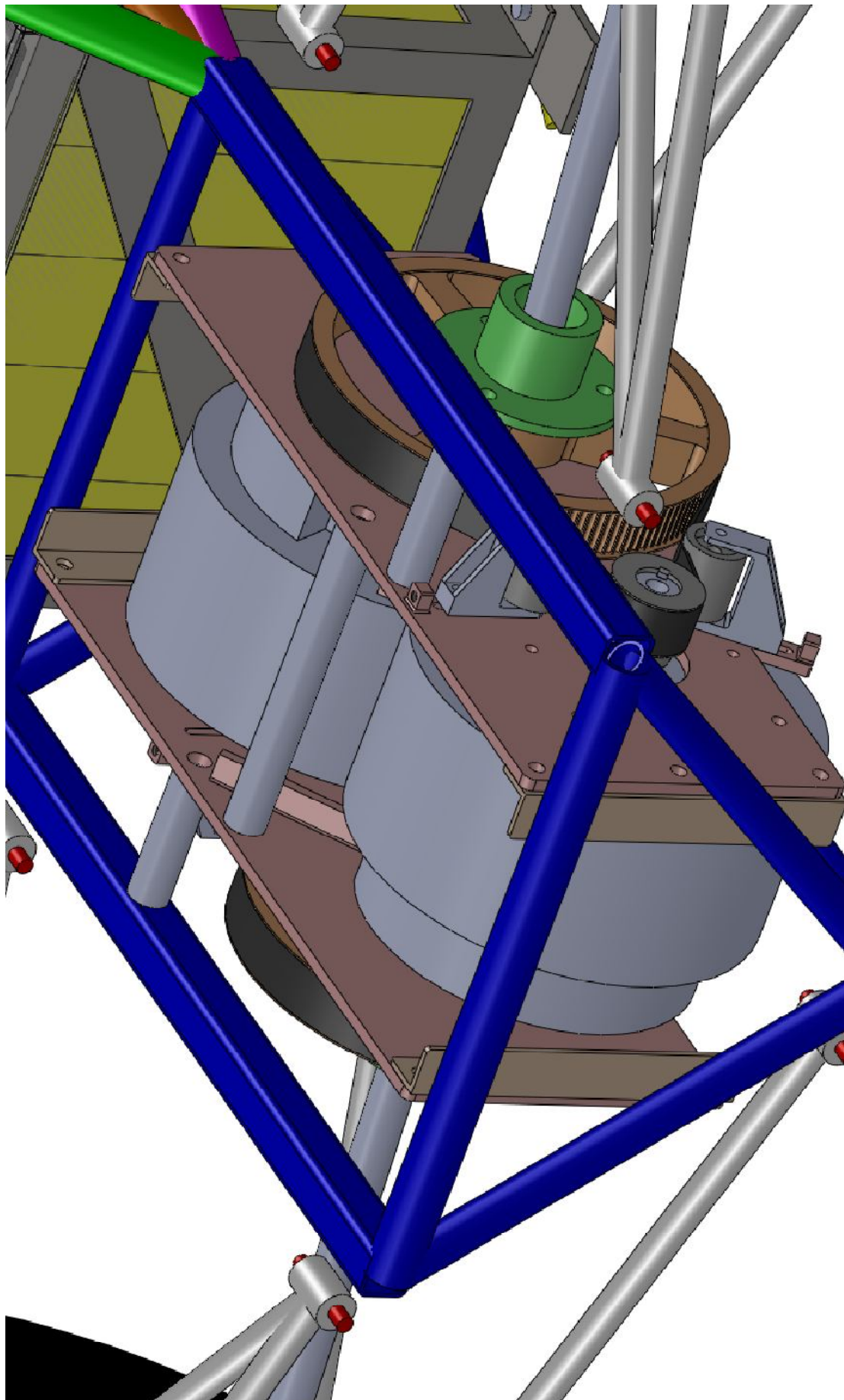
This exploded view diagram illustrates the assembly of a mechanical component, possibly a pump or motor. The parts are numbered as follows:

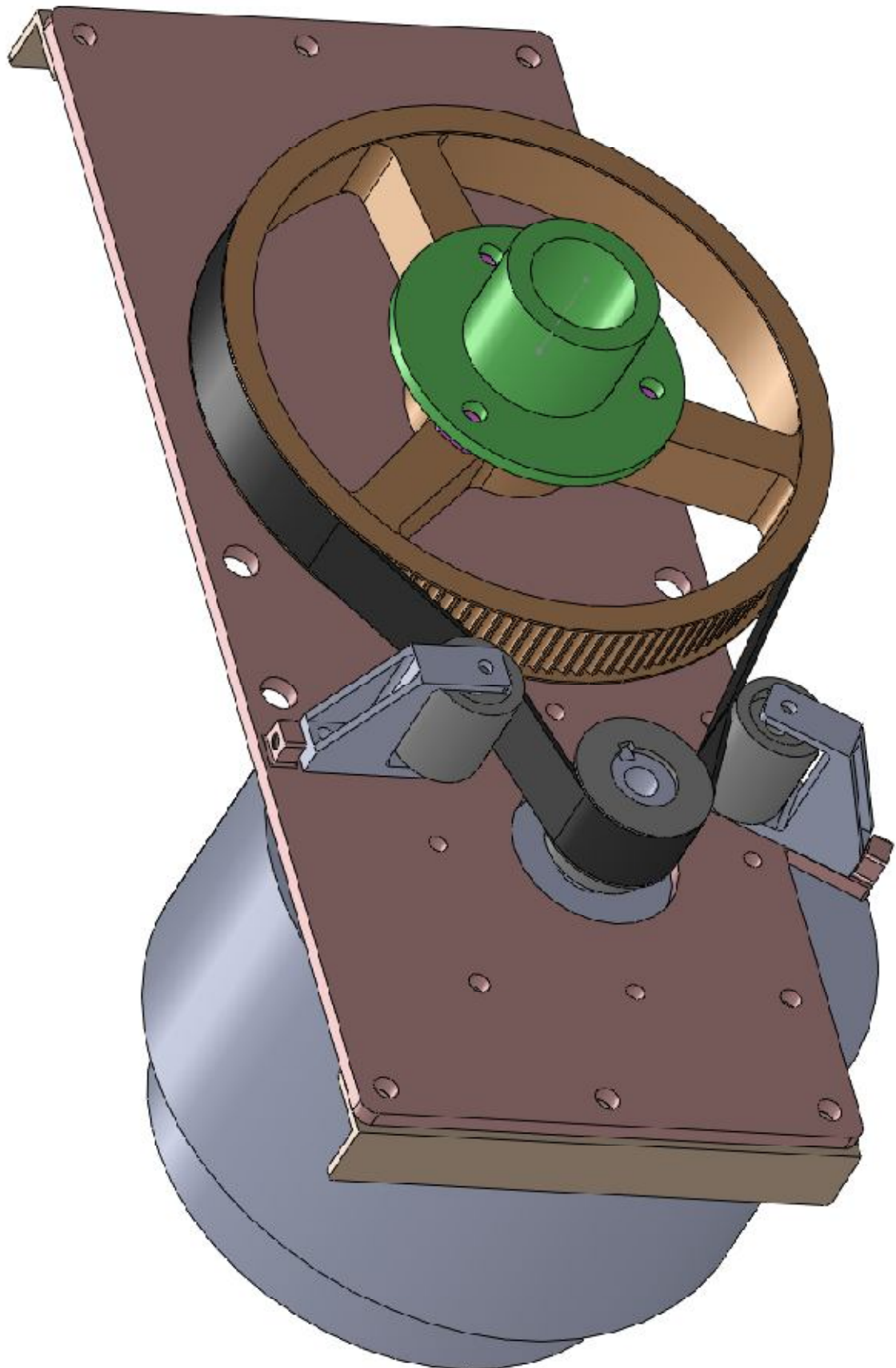
- 1. Base plate
- 2. Large gear
- 3. Small gear
- 4. Shaft
- 5. Housing
- 6. Motor unit
- 7. Flange
- 8. Bolt
- 9. Nut
- 10. Washer





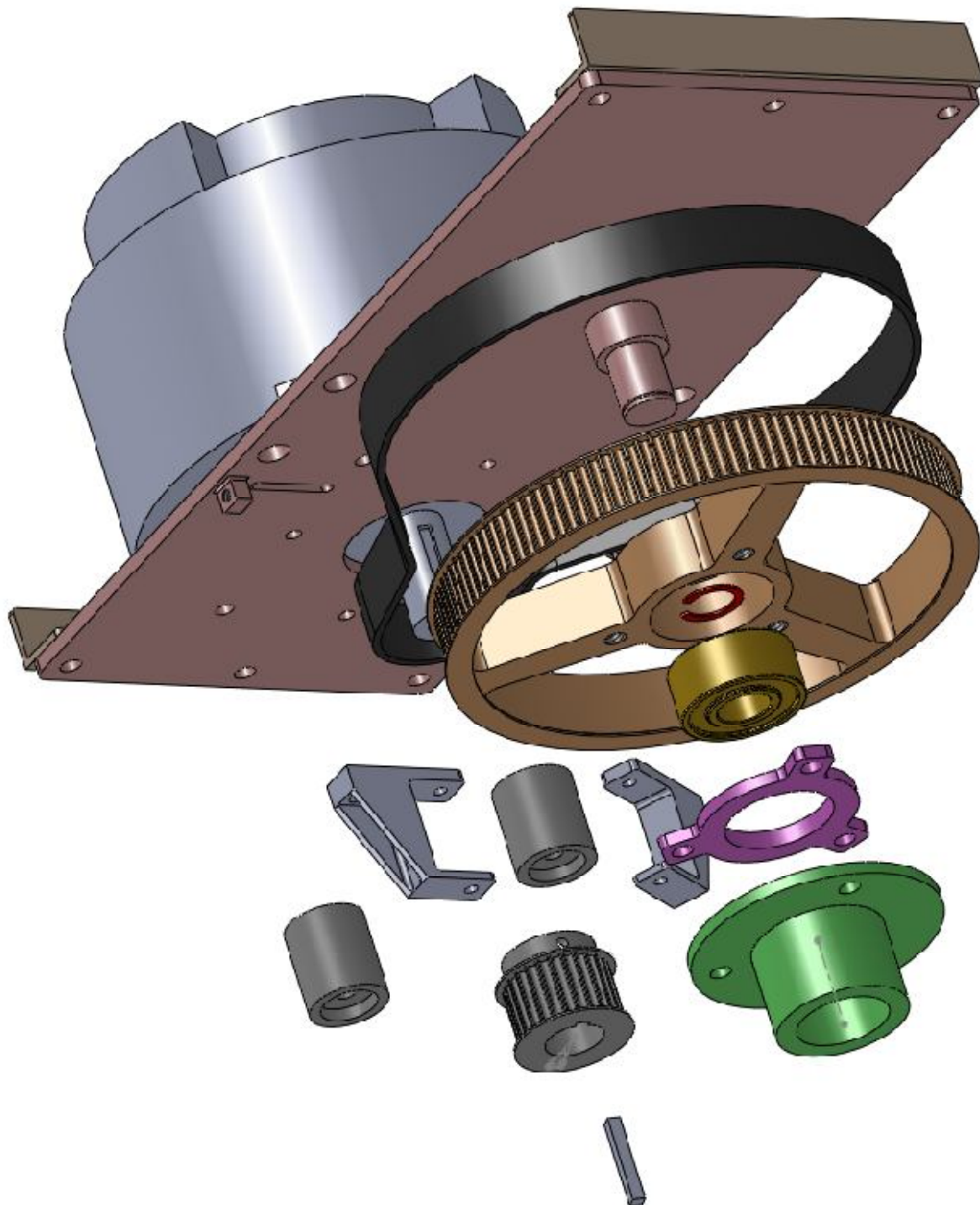
D: Inboard Design



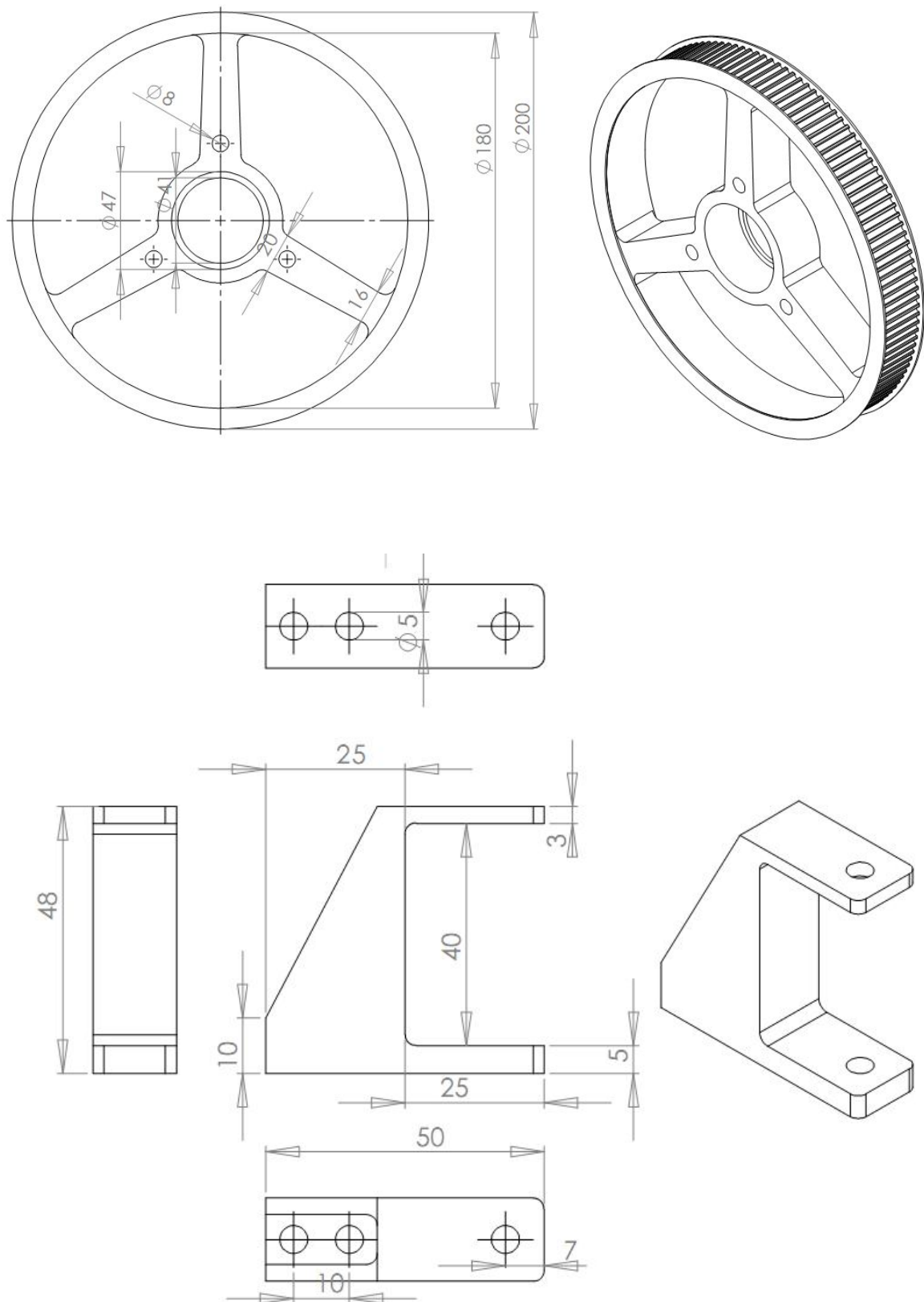




E: Exploded View of Inboard



F: Pulley & Idler



[illegible]